ANALYSIS OF THERMAL PERFORMANCE OF MULTILAYER SYSTEMS FOR FIRE DOORS

Mariana de Magalhães Moia

Dissertation to obtain a Master's Degree in:

Industrial Engineering

Mechanical Engineering Branch

November 2022

ANALYSIS OF THERMAL PERFORMANCE OF MULTILAYER SYSTEMS FOR FIRE DOORS

Mariana de Magalhães Moia

Dissertation presented to the School of Technology and Management of the Polytechnic Institute of Bragança to obtain the **Master's Degree in Industrial Engineering, Mechanical Engineering Branch** under the **Double Diploma** with the Federal University of Technology – Parana.

Advisors from Polytechnic Institute of Bragança:

Prof.º Dr. Luís Manuel Ribeiro Mesquita

Prof.º Dr. Paulo Alexandre Gonçalves Piloto

Advisor from Federal University of Technology – Parana:

Prof.º Dr. Thiago Antonini Alves

November 2022

I dedicate this work to my family.

This work was developed within the scope of the project NORTE-01-0247-FEDER-072225 "Desenvolvimento de Portas Decorativas Corta-Fogo de Madeira com Elevado Desempenho – HiFireDoor".

Acknowledgments

First of all, I would like to thank my parents Rosimere Lino and Márcio Moia for all the support, encouragement and love given throughout my life. I would also like to thank my grandfather Joaquim Lino for always valuing education. Without them I would be nothing.

I thank my housemates Arnaldo Dias, Victória Melo, Gustavo Funchal, Diogo Salvati, Bruno Marra and Daniela Elsenbach for being my home and my family during this period living in Portugal.

I would like to thank my supervisors Professor Luís Mesquita, Professor Paulo Piloto and Professor Thiago Antonini for all the support and teachings during the realization of this thesis. And I would also like to thank Professor Daniele Toniolo Dias, my Scientific Initiation advisor, for having had a great influence on my academic trajectory.

I would like to thank Engineer Luísa Barreira for her support and daily companionship in the laboratory, Engineer Matheus Alves for his teachings. I would also like to thank Djems Andrade for his company in the laboratory.

And finally, I would like to thank my friend and veteran, Adriano Krevicz for all the support he gave me from the beginning, related to both IPB and moving to another country.

Abstract

Residential fires are responsible for over 5000 deaths a year in Europe. One way to increase fire safety in homes is to use fire doors. Wood is more sustainable compared to other materials used in construction.

The present research focused on developing and analysing the reaction to fire of cork panels for a future application as the core of a fire door made of a multilayer wooden sandwich panel.

In total, ten different cork agglomerates were produced. The thickness (12 or 19 mm), the resin (MDI or TDI) and the amount of expandable, flame-retardant graphite used (0%, 5%, 10% or 20%) were varied. The samples were tested in the calorimetric cone following the EN ISO 13927 standard. Triplicate mass loss tests were performed at constant heat fluxes of 50 and 75 kW/m².

First, the influence of the thickness of the agglomerate on its fire performance was studied. The thicker panels (19 mm) showed lower HRR peak values than the thinner panels for both resins evaluated. The results allowed us to analyse that, although they present a similar behaviour, the samples made with TDI released more heat in total than the MDI samples for the same thickness and amount of graphite. It was also possible to notice that the thinner samples presented the second peak of the HRR before the thicker ones. Therefore, it was chosen to carry out the analysis of the influence of expandable graphite on 19 mm thick cork agglomerates.

Expandable graphite (EG) showed good results. Its addition reduced HRR and THR values of the specimens. The mass loss of the samples with EG was more gradual than the samples without the additive. MDI resin was shown to react better with the flame retardant.

***Keywords**:* Cork Agglomerate, MDI, TDI, Cone Calorimeter, Expandable Graphite, HRR.

Resumo

Incêndios residenciais são responsáveis por mais de 5000 mortes por ano na Europa. Uma maneira de aumentar a segurança contra incêndio em residências é usar portas corta-fogo. A madeira é mais sustentável em comparação com outros materiais utilizados na construção.

A presente investigação centrou-se no desenvolvimento e análise da reação ao fogo de painéis de cortiça para uma futura aplicação como núcleo de uma porta corta-fogo constituída por um painel sanduíche de madeira.

No total, foram produzidos dez aglomerados de cortiça diferentes. A espessura (12 ou 19 mm), a resina (MDI ou TDI) e a quantidade de grafite expansível retardador de chama utilizada (0%, 5%, 10% ou 20%) foram variados. As amostras foram testadas no cone calorimétrico seguindo a norma EN ISO 13927. Testes de tripla perda de massa foram realizados em fluxos de calor constantes de 50 e 75 kW/m².

Em primeiro lugar, estudou-se a influência da espessura do aglomerado no seu comportamento ao fogo. Os painéis mais espessos (19 mm) apresentaram valores de pico de HRR menores do que os painéis mais finos para ambas as resinas avaliadas. Os resultados permitiram analisar que, apesar de apresentarem um comportamento semelhante, as amostras feitas com TDI liberaram mais calor no total do que as amostras de MDI para a mesma espessura e quantidade de grafite. Também foi possível notar que as amostras mais finas apresentaram o segundo pico da HRR antes das mais grossas. Assim, optou-se por realizar a análise da influência do grafite expansível em aglomerados de cortiça com 19 mm de espessura.

O grafite expansível (EG) apresentou bons resultados. Sua adição reduziu os valores de HRR e THR dos espécimes. A perda de massa das amostras com EG foi mais gradativa do que as amostras sem o aditivo. A resina MDI mostrou reagir melhor com o retardador de chama.

Palavras Chave: Aglomerado de Cortiça, MDI, TDI, Cone Calorimétrico, Grafite Expansível, HRR.

Index

List of Figures

List of Tables

List of Abbreviations

Abbreviation	Explanation
EG	Expandable Graphite
EHC	Effective Heat of Combustion
EN	European Standard
ESTiG	School of Technology and Management
EU	European Union
EuroFSA	European Fire Safety Alliance
HRR	Heat Release Rate
HRpeak	Peak of Heat Release Rate
IFR	Intumescent Flame Retardant
IPB	Polytechnic Institute of Bragança
LERM	Laboratory of Structures and Strength Of Materials
MDF	Medium Density Fiberboard
MDI	Methylene Diphenyl Diisocyanate
MDP	Medium Density Particleboard
MHRR	Mean Heat Release Rate
MLR	Mass Loss Rate
OSB	Oriented Strand Board
PFP	Passive Fire Protection

PP	Polypropylene
PU	Polyurethane
PUF	Polyurethane Foam
PVC	Polyvinylchloride
TCPP	Tris(Chloropropyl)Phosphate
TDI	Toluene Diisocyanate
THR	Total Heat Released
Tign	Ignition Time
TML	Total Mass Loss
UTFPR	Federal University of Technology – Parana

Chapter 1: Introduction

1.1 CONTEXT AND MOTIVATION

Residential fires are responsible for thousands of deaths annually. Therefore, studying fire protection means is extremely important. According to the European Fire Safety Alliance (EuroFSA), it is estimated that more than 5000 people die per year from residential fires in Europe and the number of injured people is about 10 times higher, [1].

The environment is a widely discussed issue nowadays. The scarcity of resources and environmental pollution are two major problems that concern sustainable human development. Selecting natural resources for the production of industrial goods and reducing waste play a key role in the global environmental challenge. Industries are increasingly engaged in reducing the consumption of non-renewable resources and unfavourable environmental effects.

In 2018, the European Union (EU) established a goal to help reduce CO_2 emissions. The plan is to achieve an 80% global reduction in domestic carbon dioxide emissions by 2050. The European Commission's strategy is built around five objectives: ensuring food security, managing natural resources sustainably, reducing dependence on non-renewable resources, mitigating and adapting to climate change, and creating jobs and maintaining EU competitiveness, [2].

With this, the development of new fire protection means made of sustainable materials is of utmost importance. Wood is a much more sustainable and renewable material if compared to other materials used in civil construction. Steel and concrete productions are responsible for a large share of global emissions, [3]. In addition, according to the General Directorate of Economic Activities of Portugal, the wood and cork industries have great weight in the country. In 2017, it presented a turnover of 1,632.59 M€, [4].

The potential of timber is due to its production. The forest-based industry represents a circular bioeconomy. The "leftovers" - such as wood chips, sawdust, and bark - can be used in industry for the production of paper, wood-based panels, and energy generation. The final

product can also be reused after the main use and become raw material for a new product or energy source, [5].

However, the problem of wood if compared to steel and concrete is its flammability. Therefore, its fire resistance becomes something to be concerned about in its use. Cork is known for being a good thermal insulator, so it becomes interesting to study its application in civil construction to improve fire safety. The problem is that for the manufacture of cork panels it is necessary to use resins, and they are often combustible. In this way, the application of flame retardant components is well regarded.

1.2 PROPOSED OBJECTIVES

Within this context, it is necessary to observe and know the negative and positive points of each wood-based panel to find solutions for multilayer panels that can be used as thermal insulators for fire safety in civil constructions to have a more ecologically correct structure than those currently used, but without losing thermal performance.

Thus, the main objective of this thesis is the evaluation of the fire performance of agglomerated cork panels to be applied as a core of a multilayer panel for future use in a wooden fire door.

For this, the secondary objectives of the work are the manufacture of agglomerated cork panels and the analysis of the influence of the type of resin and the flame retardant used.

1.3 THESIS CONTENT AND ORGANIZATION

This work is divided into 6 chapters:

- The first chapter is the introduction, where there is a brief contextualization of the theme.
- So the second chapter is the state of the art. In this chapter, there is a deeper explanation of the subject, with several bibliographical references showing its importance.
- The third chapter has the materials and methods. In this chapter, the entire methodology used during the thesis work is described in detail.
- The fourth chapter is that of results and discussions. There, all the results are presented, analysed and compared.

- And finally, the fifth chapter is the conclusion, where the author shows the outcome and what conclusions she reached with the results of this work.

Chapter 2: State of Art

2.1 FIRE DEVELOPMENT

Since this work is an analysis of the thermal performance of multilayer systems for fire doors, it is necessary to know the fire development from its start to its end.

Fire behaviour can be described by using a temperature-time curve, [6], as shown in Figure 1. This curve is characterized by two well-defined branches: ascending and descending, [7]. It provides the temperature of the gases as a function of the fire time. From that curve, it is possible to calculate the maximum temperature reached by the structure and its capacity to resist high temperatures, [8].

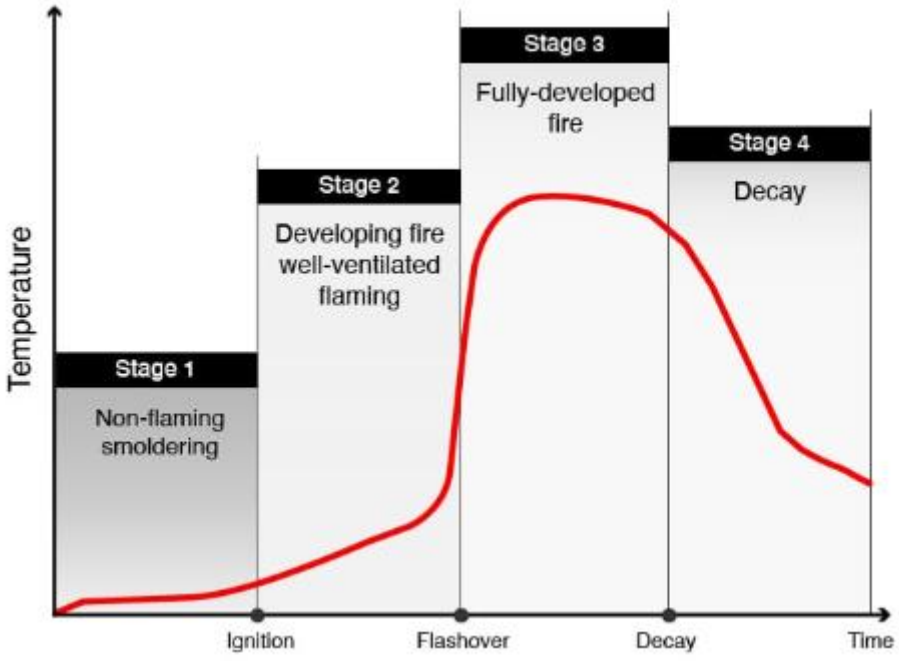

Figure 1: Temperature-time curve of a real fire, [9].

The evolution of the temperature of gases in a fire has three stages delimited by two points – flashover and maximum temperature – and starts from the ignition. The regions of a real fire curve are explained below, [7], [10]:

- **Ignition:** the instant of the beginning of the fire, of the flame. The temperature increases gradually. It is minimally influenced by the characteristics of the compartment. It does not endanger human life or the building structure.
- **Pre-flashover:** the heating stage started shortly after ignition. It is characterized by an acceleration in temperature rise. At this stage, the fire is still localized and its duration depends on the characteristics of the compartment. This stage begins and ends with the possibility of the instant known as flashover.
- **Flashover:** it's the instant after which the entire compartment is engulfed in flames. The crash is no longer controllable using active protection. The flashover is called the moment of generalized inflammation.
- **Post-flashover**: stage characterized by a sudden change in temperature growth. At this point, all the combustible material in the compartment ignites. The temperature of the hot gases exceeds 300 °C and grows rapidly until reaching the maximum temperature of the fire.
- **Decay/Cooling:** the stage that represents the gradual reduction of the temperature of the gases in the environment, after the complete extinction of the combustible material present in the compartment. There are no new fire loads to feed the flames. Then, heat loss begins, that is, the gradual cooling of the fire.

Before the flashover, the fire can be fought with so-called active fire protection, measures that need to be triggered, either manually or automatically, to work in a fire situation. They are smoke and heat detectors, sprinklers, smoke control and exhaust, hydrants, and fire extinguishers. If they are sufficient, the fire can be controlled and suppressed, without any burden on structural safety, [8]. However, passive protection is no longer sufficient to fight the fire once a flashover occurs. At this point, the fire is controlled by the fire load, until it is completely burned out and passive fire protection (PFP) is required, [7].

PFPs are measures that are incorporated into the construction of the building and do not require any type of activation for its operation. Examples: escape routes, openings in the building (such as windows and doors), proper sizing of structural elements for the fire situation and building compartmentation, [11]. This type of measure guarantees greater structural strength and ease of access to the accident site, and prevents its spread to adjacent rooms or buildings, to ensure rescue and firefighting actions.

2.2 URBAN FIRE

Urban fires are a real problem in today's society. According to EuroFSA, [12], the vulnerable community is growing. The three main groups that are included in this vulnerable community are elderly people (65+), disordered people, and children. This group suffers for not being able to be so agile when evacuating the building. Research done on 9 European countries by EuroFSA shows that more than half of the fatal victims of residential fires are people aged 65 and over.

Therefore, we need to provide fire safety in these groups of citizens' residential environment, so they won't be at a higher risk of being involved and/or suffering the consequences of a fire. If we can increase the fire resistance of building elements, we increase the time to get out of the building safely, and consequently, people will have more time to escape.

To improve de fire safety in a place, it is needed to evaluate the factors that we can or cannot change. For example, a person's age and related illness, disabilities, and socioeconomic status are factors that can't be influenced. But we can influence factors such as the fire resistance of the building and the fire prevention resources. Thermal performance is exceptional and must be considered in structural design.

The fire scenario is influenced by the following factors, [7]:

- → **compartment geometry** – a room restricted by walls, floors, setbacks, and others, which limit the spread of the fire to the surroundings;
- → **fire load** – combustible material present in the compartment;
- → **ventilation** – characterized by openings in the compartment, such as doors and windows;
- → **thermal properties of the materials that make up the compartmentalization elements.**

Due to that, one solution to improve house fire safety is delaying the flammability of the building and the fire spread. It can be done by increasing compartmentalization and using materials with better properties.

The thermal response of materials influences the severity of the accident and, the subdivision elements have the function of confining the accident to the place of origin, preventing its propagation to adjacent compartments and neighbouring buildings. Consequently, they have a huge influence on building safety, [13].

Installing fire doors is a way to provide more fire safety, once it prevents the fire from spreading to other rooms.

2.3 FIRE DOORS

Fire doors limit the spread of flame and hot gases during a certain period if correctly used, [14]. This device is a passive fire protection measure. As explained in the previous topic, it is a system that is included in the structure of the building and responds as and when the fire reaches the building's compartments and creates safe evacuation zones.

Fire doors provide compartmentation, which will contain the fire to a local area only and prevent the immediate spread of fire to neighbouring rooms or buildings, [15]. Thus, as a consequence, fire doors reduce the chances of fire growing and injuring people, both the people who were already present in the building before the fire started and the rescue team and firefighters. In other words, fire doors are key elements in fire safety once they slow or even stop fire propagation.

PFPs must be tested to determine the fire-resistance rating of the final assembly. It is usually expressed in terms of hours of fire resistance, [15]. In Europe, the standard that classifies construction products and building elements is EN 13501-2, [16] according to the results obtained in the tests performed following Eurocode 1, [17].

2.4 WOOD AS A SUSTAINABLE CONSTRUCTION MATERIAL

The versatility of wood is notorious. It is the source of a wide range of products. Its use in several fields is the result of a wide spectrum of desirable properties among the many species of wood. These properties range from appearances - such as texture, grain pattern, and colour - to machinability and physical properties such as dimensional stability, density, moisture content, thermal conductivity, and deterioration resistance. Often, more than one property is required for the application of a product.

Some of these physical properties vary by species. Others tend to be species-independent. The wood varieties generally used for the production of glued and sawn laminated wood elements, plywood and boards are the following species: *Pinus Elliott*, *Pinus Caribaea*, *Eucalyptus citriodora*, *Eucalyptus Grandis* and *Tectona Grandi*, [18].

In general, all woods have the following characteristics in common, [19]:

- The constituent elements of the trunk are symmetrical in the radial direction and predominantly vertical, as illustrated by Figure 2;
- The main chemical composition of its cells is cellulose, non-cellulosic carbohydrates and lignin;
- They are anisotropic, which means that their physical properties differ according to dimensional variations;
- They are hygroscopic, i.e., the moisture content varies with atmospheric humidity and temperature;
- They are susceptible to be attacked by xylophages, such as termites;
- They are flammable, especially when dry.

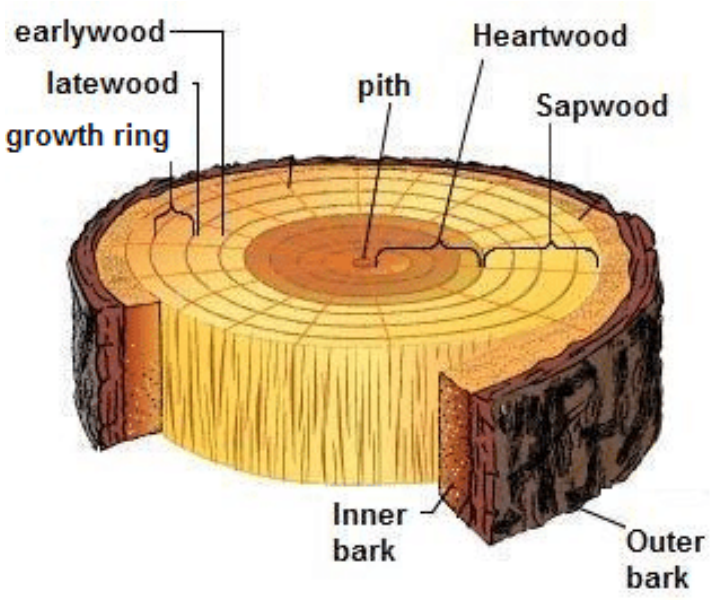

Figure 2: Cross section of a tree trunk, [20].

Santos *et al*, [21], did an integrative review on the use of wood in civil construction and measured that 18% of all the scientific texts about this theme they researched were related to sustainability.

The processing and manufacturing of steel and concrete are largely responsible for the global emission of polluting gases into the atmosphere, [22]. Therefore, avoiding using these materials can be a solution to reduce emissions.

Wood is acknowledged as the most useful sustainable material once it is renewable, carbon-neutral, has less carbon dioxide produced, has low energy consumption, is durable, non-toxic, and is naturally abundant, [23], [24]. This resource is largely used nowadays as fuel and as raw material in civil construction and transport. As a result of it, wood is an important input to the world economy, [25].

The use of wood in civil construction dates back to the dawn of civilization, [26] due to its large availability in nature, [21]. An advantage is that in addition to being a good raw material for civil construction and being a renewable resource, it has a good aesthetic, [27].

Wood presents good structural behaviour in fire situations, however, as it is a combustible material, it is frowned upon.

2.5 DEFECTS OF WOOD

One of the flaws of wood for construction is that wood and its products can lose their physicochemical properties chemical over time. It happens due to weather conditions, temperature, humidity, ultraviolet radiation, rain, snow, or even insects, bacteria, and/or fungi infestation.

Another factor that can compromise the integrity of wood properties is the fact that it is the result of the growth of a living being. Thus, there may be heterogeneities according to the environment in which the tree for its production is cultivated. In addition, during the wood drying process, defects such as cracks and warping may occur, [24].

But the biggest problem with wood in civil construction when talking about fire safety is that wood is a combustible material.

Although, when exposed to high temperatures, it does not melt or warp like steel elements or spall like concrete. Wood combustion is slow and superficial. While the external layer buns, the central core of the section can remain intact, strong, and stable, [28]. This characteristic allows timber to be able to maintain the mechanical properties of the element.

2.6 CORK AS A SUSTAINABLE AND LIGHTWEIGHT CONSTRUCTION MATERIAL

Cork is a renewable, recyclable and high-performance eco-friendly material. It is the outer layer of the bark of the cork oak (*Quercus Suber L.*) and is sustainably extracted from its trunk at periodic intervals (generally every 9 years), without compromising the health of the plant, [29]. Therefore, it is considered a sustainable material with a good ecological footprint, [30]. In Figure 3 it is possible to visualize the cork oak being peeled to obtain the cork.

Figure 3: Cork oak being peeled off, [31].

Regarding its mechanical properties, cork presents the typical behaviour of cellular materials: non-linear to compression. The stress-strain curve is characterized by a short linear elastic region (up to about 5% of normal strains), followed by a large plateau region (up to

~50%), corresponding to the progressive buckling of the cell walls, until their collapse in high strains (~70%) with consequent densification of the material, [30].

This material has a closed-cell alveolar microstructure, and suberin and lignin as the two main components of its chemical composition. These factors make cork a lightweight material (density varies between 120 and 240 kg/m3), [32], [33], wear-resistant, hypoallergenic, durable, [32], resilient, [29], [32], impermeable to gases and liquids with remarkable thermal and acoustic insulation properties fire retardant, [29], [32], [33], with low thermal conductivity, [29], and good damping capabilities, [33].

Cork products can be divided into two groups: natural cork and composite cork products. The first is made with cork *in natura*, in the way it is extracted, as the name implies. Typically, it is geared towards the production of wine corks. However, this production generates a lot of material waste. Then, the cork left over from the production of stoppers is crushed and becomes raw material for new composite cork products, [32].

Agglomerated cork composite panels are an example of a composite cork product. They are a result of a process of agglutination of cork granules. It requires the action of pressure, temperature, and a binder material, [34]. These agglomerates can be employed alone or in multilayer products, [35]. They can be used as a core in sandwich structures to provide thermal, electrical, and acoustical insulation without significantly contributing to the weight of the structure. Cork has several applications in civil construction, aerospace, footwear, and decoration, [34].

2.6.1 CORK AGGLOMERATES

Cork agglomerates are made by putting a mixture of cork granules with polymeric resin under pressure at a certain temperature for a certain period, [33]. The required pressure, temperature and time to produce the board depends on several factors based on the properties of the resin and/or other additive used, the mould size, the agglomerate density, and the presence of water in the mixture.

To produce agglomerated cork, it is first necessary to crush the cork into small grains of a certain size and then mix them with a binder (usually a thermosetting resin). After this phase, the mixture must be placed in a mould where the resin will cure and the mixture will harden,

forming the agglomerate plate. The resin curing process can be carried out through different techniques such as resin transfer moulding, vacuum bagging, compression moulding and spray lay-up, [30].

The most used technique is compression moulding, as it has a high reproducibility rate, [36]. This process is characterised by a mould, usually metallic, with a cavity where the mixture of cork granules and resin is distributed uniformly, and a lid that is used to press the sample. Once the cork and resin mixture is already placed in the mould, this set is compressed in a hydraulic or pneumatic press under a certain pressure and temperature until the resin is cured.

This manufacturing process allows the production of chipboard of different sizes. The agglomerated cork block can take any shape depending on the application in question, later through machining processes, [30].

According to Delucia *et al*, [30], the properties of cork-based composites depend on parameters such as the quality, quantity and granulometry of the cork in the mixture, the quantity and type of resin, and the parameters of the moulding process.

2.7 WOOD-BASED PANELS

A solid wood sheet is often financially unfeasible. As a result, research have being done to seek alternatives, [37]–[40]. One of the options was the development of wood-based panels. This way, it is possible to use the waste from the wood industry, a fact that is in constant evidence today, [41]. The choice of wood species for the production of particleboard must be based on some important parameters such as density, pH, and extractives, [40].

The engineered wood-based panels that stand out are:

- Plywood;
- Oriented Strand Board (OSB);
- Medium Density Particleboard (MDP).

They serve as alternatives to the use of lumber in civil construction.

2.7.1 SANDWICH PANELS

A multilayer panel can be classified according to the particle distribution system. It can be homogeneous, have 3 or 5 layers, or be gradual, [39]. Sandwich structures have 3 layers, see Figure 4. They are gaining huge importance in civil construction, once it combines the high strength and stiffness of the material used in face sheets with the lightness of the core, ensuring a high stiffness-to-weight ratio and good structural performances. Then, they are gaining huge importance in civil construction. The selection of the right core material is a key point in the production of sandwiches to optimize the mechanical performances and weight of the structure, [42].

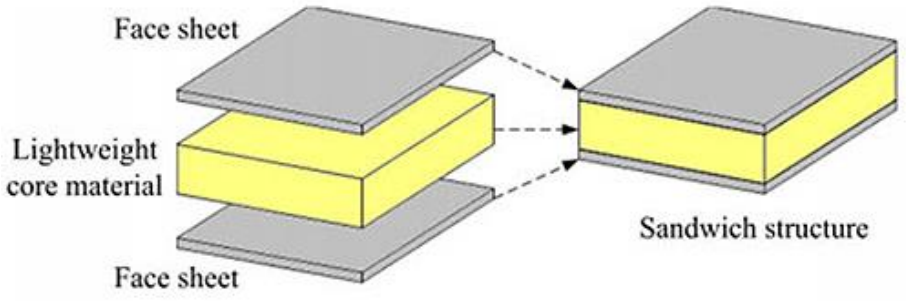

Figure 4: Main Components of Sandwich Structures, [43].

2.7.1.1 Core of a multilayer panel

Synthetic cellular materials are usually used as cores for sandwich structures due to their high-energy absorption ability, [44]. And the polymers that are commonly used: polyurethane (PU), phenolic, polystyrene, and polyvinylchloride (PVC) – traditional used to obtain core foams – and polypropylene (PP), Nomex, and aluminium – usually employed to produce honeycomb structures, [42].

However, despite the good performance, these material presents environmental problems and then it turns necessary to investigate new sustainable alternatives. A core material made from a biological base, such as cork, allows for a reduction in the carbon footprint of its production, the emission of greenhouse gases and the consumption of energy and chemicals. Another fact that makes it more sustainable is that it allows total or partial biodegradation of the sandwich structure at the end of its life cycle, [42].

A natural cellular material that can be used as a core in sandwich panels is cork. In addition to its thermal and acoustic insulation qualities, the use of agglomerated cork makes it possible to use the residue from the production of wine stoppers, so it reduces the waste.

In 2001, researchers from the Norwegian Institute of Wood Technology, [45] analysed the strength properties of glued laminated beams before and after fire exposure. The results showed the influence on the behaviour of the beams during and after fire exposure of the adhesives tested – Polyurethane (PU), Urea-Formaldehyde (UF), Polyvinyl Alcohol (PVA), and Emulsified Polymer Isocyanate (EPI) – was small. They observed no difference in charring rate during the fire and in shear strength after a fire. But, it is important to mention that the sample was not loaded during the test, and a large proportion of the glue was not exposed to elevated temperatures.

However, Klippel *et al*., [46] did a comparison between the study made by Källander & Lind in 2001 and a study made König et al. in 2008 in Canada about glued laminated timber beams with finger joints in the outer lamella on the fire-exposed tension side were tested by, and they realized that on the contrary of the first one, the research made on Canada has presented that in fire situation beams with Polyurethane Reactive (PUR) and Melamine Urea-Formaldehyde (MUF) adhesives in the finger joints exhibited bending resistances of only 70 to 80 % of the bending resistance of the beams with Phenol-Resorcinol-Formaldehyde (PRF) bonded finger joints, whereas that in normal ambient situations there was no such difference.

Two resins that are commonly applied to cork are diisocyanate-based pre-polymers adhesives. One is based on methylene diphenyl diisocyanate (MDI) and the other is toluene diisocyanate (TDI). They were denoted as hard and flexible, respectively, [47].

2.8 FLAME-RETARDANTS

Exploring a flame retardant method is interesting since although cork has a good reaction to fire, resins are generally a combustible material.

There are two types of flame retardant methods which are usual in the industry. The first one is the surface treatment of the material using a coating, but this can significantly increase the final density and production costs of the agglomerates. The other is to add flame retardants to the panel mix. This is usually a simple and cheap process, [48].

A flame retardant widely used in Europe is TCPP (tris (chloropropyl) phosphate). It is usually used to increase PUFs (Polyurethane Foams) fire performance [49]. However, it is a halogenated flame retardant, and in the field of flame retardant research, halogen-free technologies have been sought after, especially intumescent flame retardant (IFR). This is due to the fact that materials containing halogen flame retardants release ambiguous, corrosive, toxic, and carcinogens smoke during combustion, [48]–[50].

2.8.1 EXPANDABLE GRAPHITE

Expandable graphite (EG) is an IFRs. It is an intercalation compound of flaked graphite. Studies have shown that it exhibits excellent flame retardant characteristics, [50]–[55]. When exposed to a heat source, the EG expands and generates a voluminous insulating layer on the polymer surface, providing flame retardant properties. Its expansion process starts around 240ºC and its volume can increase by more than 20 times, depending on the granulometry, [57].

In recent years, EG has been successfully used as a flame retardant for a wide range of polymers with satisfactory results. Experimental results showed that the addition of EG in PUF significantly reduces the values of the heat release rate and the total heat released during tests on the cone calorimeter, [48], [52]. Zheng *et al*., [53], also showed that expandable graphite improves polypropylene (PP) fire performance. In contrast, [54], studied its effect on an epoxy resin. There was an increase in the ignition time, but the EG showed an increase in the peak value of the heat released rate. The total heat released and the effective heat of combustion did not change.

2.9 EXPERIMENTAL DESIGNS

Experimental design is extremely important in academic research so that the experimenter can draw conclusions from their results. These methods are based on statistical principles, and by using them, researchers can extract the maximum of useful information from the system under study, performing a minimum number of experiments, [56], [57].

There are several techniques available to improve or optimize systems, processes and products. When it is necessary to evaluate more than one variable at the same time, with statistical reliability of the results, the factorial design has been widely used, [58]–[63], in the most diverse experiments.

2.10 EVALUATION OF FIRE RESISTANCE

One of the main causes of the failure of structural elements of wood and its derivatives occurs is the reduction of the resistant cross-section during fire exposure, [64]. This reduction can be calculated from the carbonization rate, [65].

Experimental results show that there is a linear (approximately) relationship between charring time and the depth from the original surface to the isotherm of 300°C, [65].

The tests that need to be done on the panel to be used as a building element are specified by Eurocode 1, [17]. According to the results, the panel must be classified based on EN 13501-2, [66].

Heat release rate (HRR) is the rate of energy released by the material per unit of surface area. It is a parameter of great importance, as it indicates the potential fire risk and combustibility of a given material. Thus, the lower the HRR, the lower the fire risk offered by the material. The HRR of a material can be determined by tests performed on a Cone Calorimeter, [67].

2.10.1 CONE CALORIMETER

The Cone Calorimeter is currently the most advanced method for evaluating the reactions of materials to fire, [67]. Its name is due to the conical shape of the radiant heater that produces an almost uniform heat flux along the surface of the sample.

The equipment is used to carry out small-scale tests of reaction to fire of materials standardized by EN ISO 13927, [68]. This standard specifies a method for evaluating the HRR of a sample exposed to controlled levels of irradiance ranging between 0 and 100 kW/m². For this, according to the standard, the products to be tested must be essentially flat in horizontal orientation. The surface of the specimen must have an area size of at most 100 x 100 mm² and a thickness between 6 and 50 mm. Typical irradiance levels used are 25, 35, 50 and 75 kW/m², [69]–[74].

The HRR is evaluated by measuring the output of a thermocouple located in a chimney above the burning sample subjected to a known heat flux from a conical heater. The output (in mV) is converted into an actual rate of heat per unit area (in kW/m²). Ignition time (sustained

flame) is also measured in this test. The mass loss of the sample can also be optionally measured by continuously recording the load cell output.

The equipment software also displays the Mean HRR (MHRR), the peak HRR (HRRmax), the Total Heat Released (THR), the Total Mass Loss (TML), the Mass Loss Rate (MLR), Effective Heat of Combustion (EHC), Ignition Time (Tign) and Flameout.

Chapter 3: Materials and Methods

This chapter discusses the materials and methods used in this work to analyse the thermal performance of the multilayer systems for fire doors. All this work was developed in the Laboratory of Structures and Strength of Materials (LERM), located at the School of Technology and Management (ESTiG) of the Polytechnic Institute of Bragança (IPB),

Foremost, before evaluating the performance of a system, it is necessary to define and create this system.

3.1 FACTORIAL DESIGN

Once the objectives were defined, an experimental strategic planning methodology is important to optimize the process. Factorial design was the method chosen. It is largely used in studies that involve many variables, [57], which is the case of this work, since there is variation in thickness, resin and amount of flame retardant in the panel. Planning is important because it makes it possible to carry out the minimum number of experiments required in an organized manner. In this way, it optimizes time and reduces the consumption of resources, [75]. It is a useful analytical strategy and its main application is the screening of the most relevant variables of a given analytical system, [57].

To carry out a factorial design, it is first necessary to specify the levels at which each factor will be studied. These factors can be quantitative values or qualitative versions to be evaluated in the experiment, [56].

It is necessary to vary a factor and observe the consequence of this variation to study its effect on the final result. This implies that it is necessary to carry out tests on at least two levels for each facto. The design in which all variables are studied at only two levels is called 2^k factorial design. In this method, there are k factors, that is, k variables controlled by the experimenter. It is necessary to carry out $2 \times 2 \times \ldots \times 2 = 2^k$ different tests, [56], hence the name.

In this work, it will be evaluated how the thermal performance of the system will depend on three factors: type of resin, and thickness of the cork agglomerate of the core. With that, k=2. That is, the complete factorial design will need to perform $2^2 = 4$ trials for each type of analysis.

To evaluate the influence of the thickness and the pure resin, the levels are:

- cork agglomerate thickness: thinner and thicker;
- resin: MDI and TDI.

The listing of these combinations, which is called the planning matrix, is presented in Table 1. It lists the attempts in the standard order: the columns start with the lowest level (-) and then the signs alternate. One by one in the first column, - + - +..., then two by two, - - + +...., [57].

Table 1: Planning Matrix for pure agglomerates.

		Lowest Level (-)	**Highest Level (+)**
Factors:	**A → Resin**	MDI	TDI
	B → Cork Agglomerate Thickness	Thinner	Thicker

Composition	**Resin**	**Thickness**
1	MDI	Thinner
2	TDI	Thinner
3	MDI	Thicker
4	TDI	Thicker

In this way, factorial design allows the combination of all possible factor levels. Thus, the effect of each factor could be evaluated according to the change in the response when passed from the - level to the + level of that factor.

The same was done to define the use of expandable graphite after having already evaluated which thickness have better fire performance and was chosen for the panels. Table 2 declares the planning matrix for the samples with EG.

Table 2: Planning Matrix for samples with EG.

		Lowest Level (-)	**Highest Level (+)**
Factors:	**A → Resin**	MDI	TDI
	B → % of EG	5%	10%

Composition	**Resin**	**EG Weight Fraction**
5	MDI	5%
6	TDI	5%
7	MDI	10%
8	TDI	10%
9	MDI	20%
10	TDI	20%

3.2 SAMPLES NOMENCLATURE

Then, with the composition defined, it was created a pattern to the samples nomenclature. The first section represents the type of resin used (MDI or TDI). Then, the second one identifies the thickness of the core. The third one is the percentage of expandable graphite. And the last section is the number of sample of that specific composition. For example: MDI-6mm-10%EG-S3 is the third sample of MDI agglomerate with thickness of 6 mm and 10% of expandable graphite.

When referring only to a composition and not to a specific sample, the last part is removed. For example: MDI-6mm-10%EG.

3.3 AGGLOMERATED CORK PANELS

Cork grains were supplied by Granorte® in two different particle sizes: 0.2 - 0,5 mm and 3 - 4 mm, from now on denoted small and large grains respectively. The proportion of cork particle sizes used was: 6% of small grains and 94% of large grains. The small grains were placed only to envelop the larger ones and improve the adhesion between the them.

And binders, two different diisocyanate based pre-polymers, were provided by Flexpur (Ovar, Portugal). One of them was a methylene diphenyl diisocyanate (MDI) binder and the other one was toluene diisocyanate (TDI). The second one have been previously reported to be more flexible than MDI-based ones, [76]. Usually, the resin weight fraction is around 10% in cork-based agglomerates. It corresponds to a volume fraction of about 2%, [30]. And so it was done. Each resin was used separately.

3.3.1 MATLAB CODING TO DEFINE PRESS PARAMETERS

One of the issues perceived during the manufacture of the agglomerates was how to define the amount of mixture and the necessary pressure to obtain a panel with any desired thickness and density. So, it was decided to create a code in MATLAB software in which the inputs were density and thickness, and the output was pressure to be applied and the necessary amounts of each component of the mixture.

For this, a study was made of the relationship between of these four parameters. Panels were made with different pressures and quantity of mixture. These values, with the final panel thickness and it average density, were placed in a spreadsheet of Origin software. Then, graphs were plotted and, with the use of "fitting" tool of the software, the equation that relates the parameters was found.

In this way, it was possible to create a code that calculated the pressure and quantity of the components needed for each desired agglomerated cork panel.

3.3.2 COMPONENT WEIGHING

In order to manufacture the panels, each component had to be weighed first. For that, the scale was reset to zero with the container in which the material was going to be placed, then the materials were weighed, as shown in Figure 5. The amount was in accordance with the desired percentages of each component in an agglomerate cork board, defined above, and with the dimensions of the mould. Water was added in a small quantity to reduce the resin's viscosity and facilitate the process of adhesion to the cork grains.

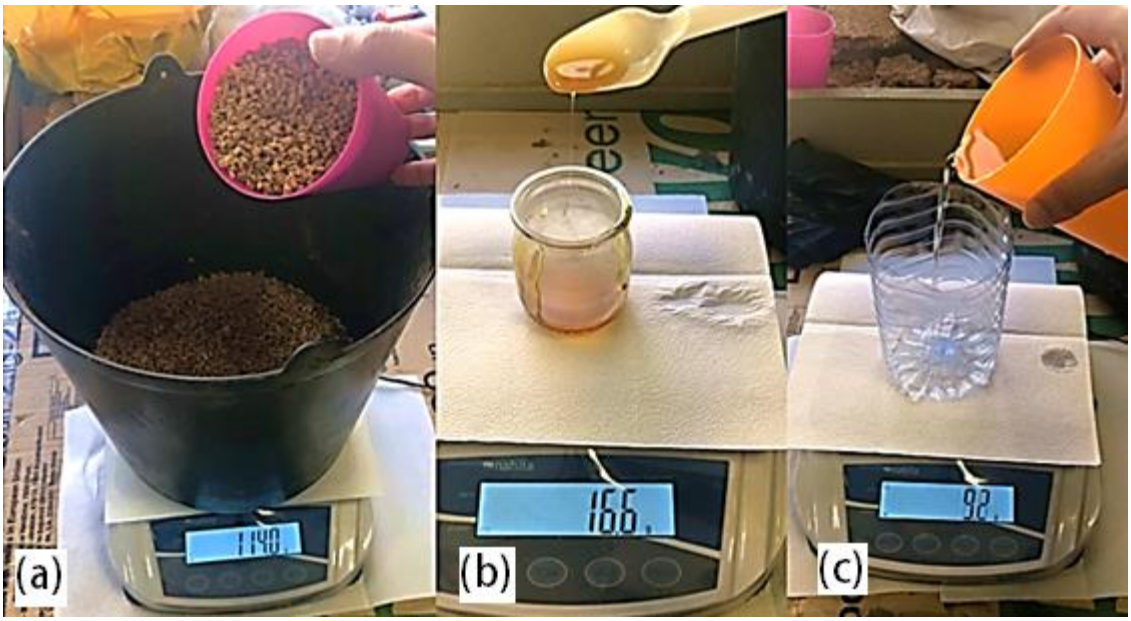

Figure 5: Weighing the materials for the manufacture of agglomerated cork. (a): cork weighting; (b): MDI resin weighting; (c) water weighting.

3.3.3 MIXTURE PREPARATION

Then, once all the materials were already weighed, the mixture was made. For this, as shown in Figure 6, they were all placed in the same container and then, with the aid of a mixer coupled to a manual drill, the components were mixed. From time to time, the equipment was paused and, wearing gloves, a mix was made manually to bring the cork granules from the bottom of the container to the surface and ensure that everything was mixed evenly.

Figure 6: Mixture preparation for the manufacture of agglomerated cork.

3.3.4 MIXTURE MOULDING BEFORE PRESSING

Following, the cork and resin mixture is placed in the mould.

3.3.4.1 Smaller Mould

At first, it was used a metallic mould with base dimensions 165 x 165 mm and 90 mm high. This size required the use of a small amount of mix material. In this way, the waste of raw material was reduced until it reached the ideal mixture and parameters values for the cork agglomerates.

The mould was previously lined with tracing paper, so that the sample does not stick to the mould, as shown in Figure 7.

Figure 7: Mould filling for making an agglomerated cork.

Then, wearing gloves, a manual levelling was done so that the compound was evenly distributed in the mould, illustrated in Figure 8, and thus guarantee a homogeneous sample. This whole process had to be done quickly (under 30 minutes), because once any of the resins were mixed with water, it reacted and started its curing process.

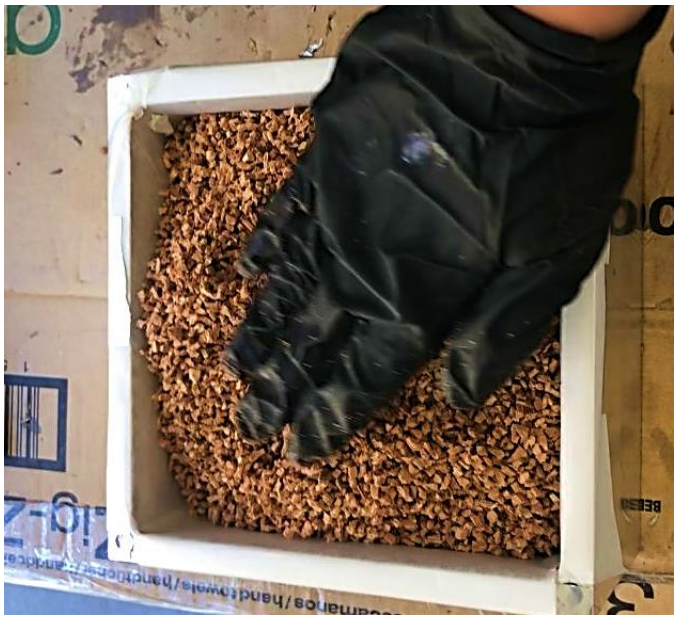

Figure 8: Manual levelling the compound.

Finally, the material was covered with a sheet of tracing paper and then the mould was closed, Figure 9.

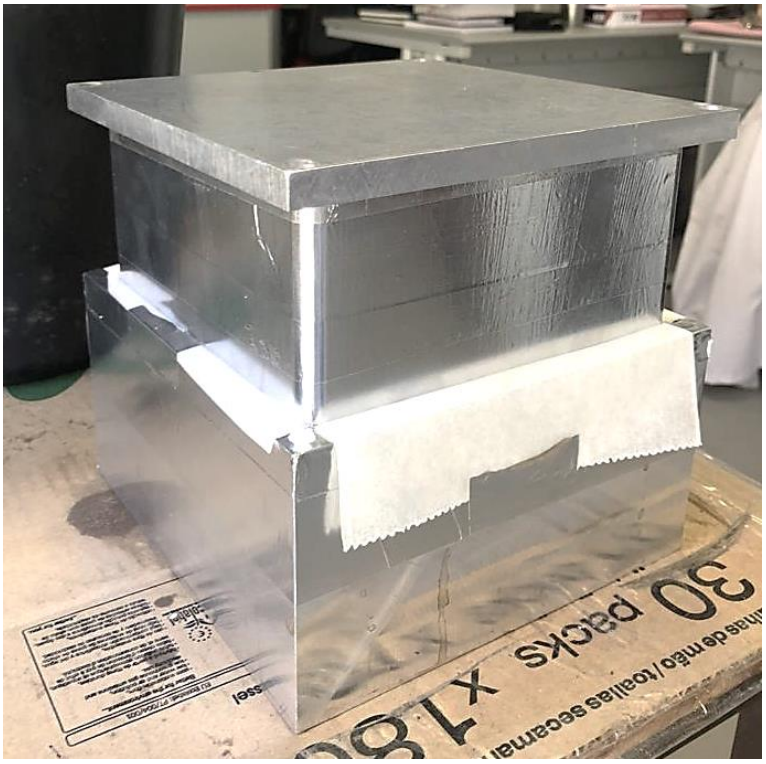

Figure 9: Closed mould.

However, this mould was too small and with that the production of the samples would take too long. In addition, a larger mould would allow larger samples and, as a consequence, larger scales tests.

This mould allowed only one sample, that would have to be cut, for testing in the calorimetric cone, which is a small scale test.

3.3.4.2 Larger Mould

Then, once the quantities of the mixture components and all the parameters would be used during the pressing were defined, it was possible to use a larger mould. This mould, Figure 10, was built in wood due to the availability of this resource at LERM, the laboratory where this work was carried out. It internal dimensions was a base of 550 x 550 mm and 80 mm high.

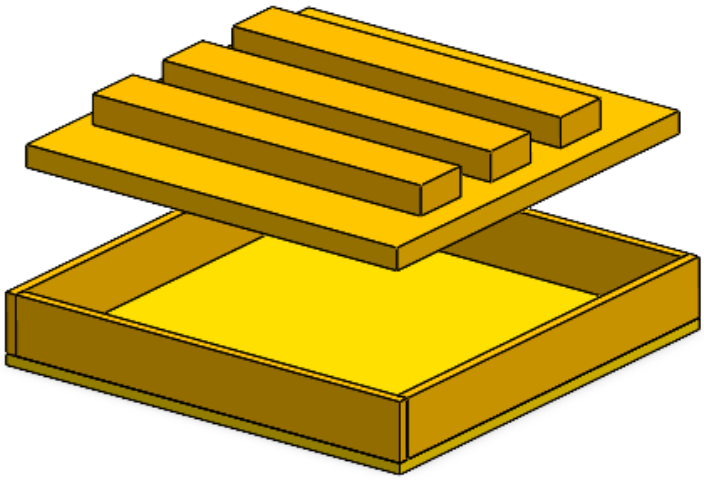

Figure 10: mould design for medium scale samples.

The whole process of putting the mixture in this mould was similar to the small one. The difference is that the base and the inner sides of the this one were coated with aluminium adhesive tape to waterproof the mould and thus prevent resin absorption by the wood.

This mould allowed 25 samples for tests in the calorimetric cone or one sample for tests in the fire simulation oven on a medium scale per panel made of agglomerate.

3.3.5 APPLICATION OF PRESSURE AND TEMPERATURE IN THE MOULD FOR PANEL FORMATION

Quickly the assembly had to be placed in the hot press, previously configured and heated, to compress the mixture and form the agglomerate, and cure the resin, Figure 11. To perform this procedure, the press was lined with aluminium foil so that it would not run the risk of being damaged by resin leakage, if any.

Figure 11: Pressing process.

To carry out this process, the MonTech LP 3000 Laboratory Press, was used at 2 MPa for 90 min at 140 ºC and 125 ºC, at first, for the samples made with MDI and TDI, respectively.

These values were chosen after a literature search. The curing temperature of the MDI resin is provided by the manufacturer. However, a literature search was necessary to find

baseline values of pressure to be applied, [30], [40], [77]–[79], curing temperature of the TDI resin, [47], [76], [80], [81], and polymerization time of both resins, [47], [80].

3.3.6 REMOVAL OF THE FINISHED AGGLOMERATE FROM THE MOULD

3.3.6.1 Smaller Mould

After completing the pressing time, the set was removed from the press. However, the demoulding could not be done immediately, since the mould, being metallic and being subjected to high temperature, dilated and made it very difficult to open.

A fan was used to accelerate the cooling through forced convection, Figure 12. With it, it took about 2 hours for the mould to reach a temperature where it was possible to open it.

Figure 12: Cooling the mould.

To open the mould, it was turned upside down and lifted. The lid, being made of solid aluminium, was much heavier than the base, so it was expected until the lid came down completely. Then the cork agglomerate could be removed.

3.3.6.2 Larger Mould

The cooling process of the medium-scale agglomerate was similar to the first. The assembly was also removed from the press to cool. Unlike the metallic one, the lid was removed from above. Then, a thin sheet of metal was passed between the sides of the panel and the mould to ensure that the chipboard was all loose and the base of the mould was turned upside down so that the panel came out.

3.3.7 SMALL SAMPLES PREPARATION

Once the panels were made, they were cut with a circular saw so they fit the dimensions of the standard EN ISO 13927, [68], to perform the cone calorimeter test. The specimens shall be square with sides measuring 100 mm ± 2 mm. For this, squares with such dimension were drawn on the panel, Figure 13. The edges were discarded for standardization of the samples.

Figure 13: Agglomerated cork panel ready for sample cutting.

3.4 CONE CALORIMETER TEST

In this work, the Cone Calorimeter equipment existing in the Laboratory of Structures and Resistance of Materials (LERM), located at ESTiG from IPB, was used. The equipment is shown in Figure 14 and it essentially consists of a smoke extraction system (1), a thermopile (2) housed by a chimney (3), a cone-shaped radiant heater (4), a specimen holder (5), and a load cell (6).

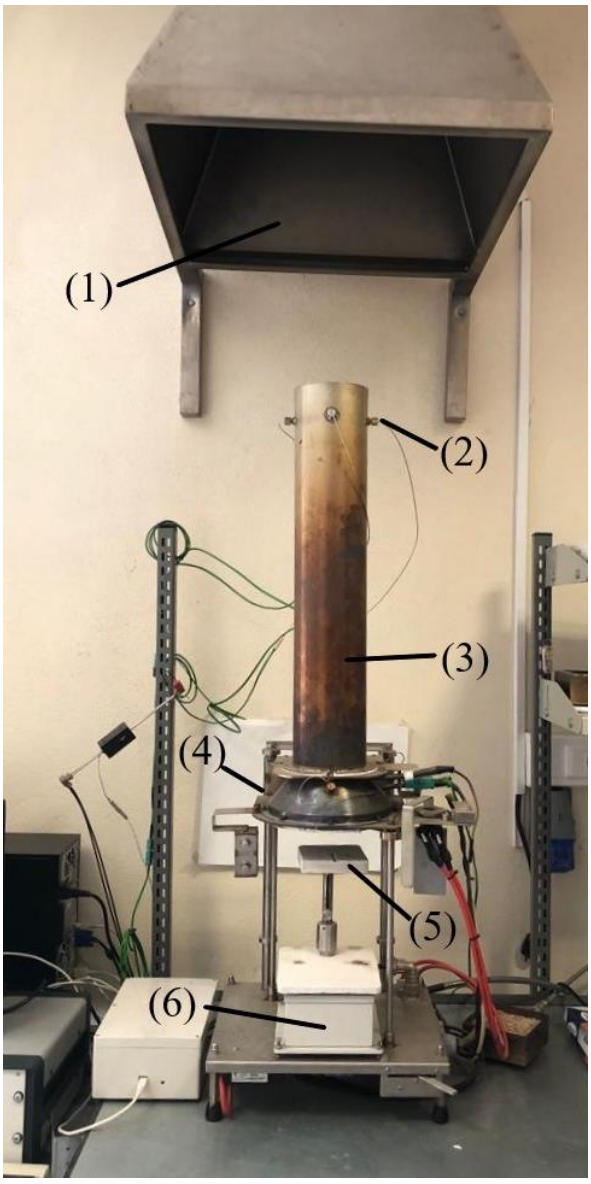

Figure 14: Cone Calorimeter.

To carry out the tests of this work, the equipment was adjusted to constant heat fluxes. The face of the sample had to be exposed at a distance of 25 mm from the cone.

3.4.1 SAMPLE WEIGHTING AND SELECTION

For mass loss testing, all samples were weighed and then a selection was performed so that all specimens tested in a certain flow had approximately the same mass. This helps to standardize the tests and gives more credibility to the results.

3.4.3 SAMPLE WRAPPING

The required specimens wrapping. EN ISO 13927, [68], says that the unexposed surfaces of the samples must be wrapped in a singles layer of aluminium foil, Figure 15. This was done to leave only the face where the flux would be applied exposed. With this, the heat release by the faces of the specimen that were not exposed to the flux would be as little as possible. In addition, this wrapping prevented any particle that is released by the sample from falling off the balance. Thus, ensuring that the test did not present a loss of fictitious mass, thus making the test even more accurate.

Figure 15: Sample wrapped in aluminium foil before testing.

3.4.4 SAMPLE HOLDER PREPARATION

Before performing the test, it was necessary to place the substrate in the sample holder. Ceramic fiber was used. For this, it was necessary to follow some steps, [66]:

1. place the retainer frame on a flat surface facing downwards;
2. insert the specimen wrapped in aluminium foil into the frame with the exposed surface facing downwards;
3. place layers of ceramic fiber mat (nominal thickness 13 mm) on top of the specimen until two layers extend above the edge of the frame;
4. fit the sample holder in the frame on top of the ceramic fiber and press down;
5. tighten the screw until the assembly was closed.

3.4.5 EQUIPMENT CALIBRATION

Each day that a test must be performed, it is necessary to verify that the equipment is in compliance. Otherwise, a new calibration is required.

The daily check started with the load cell. With the cone still at room temperature, its zero must be set and then a standard weight must be calibrated in the cone's calorimetric software.

Then it was possible to check the heat flux. The cone should be adjusted to heat up to the temperature corresponding to the desired flux. This temperature was the one set in a previous calibration. When the cone reached this temperature, the flux meter was placed at a distance of 25 mm from the base of the cone. A ruler was used to measure this distance, see Figure 16.

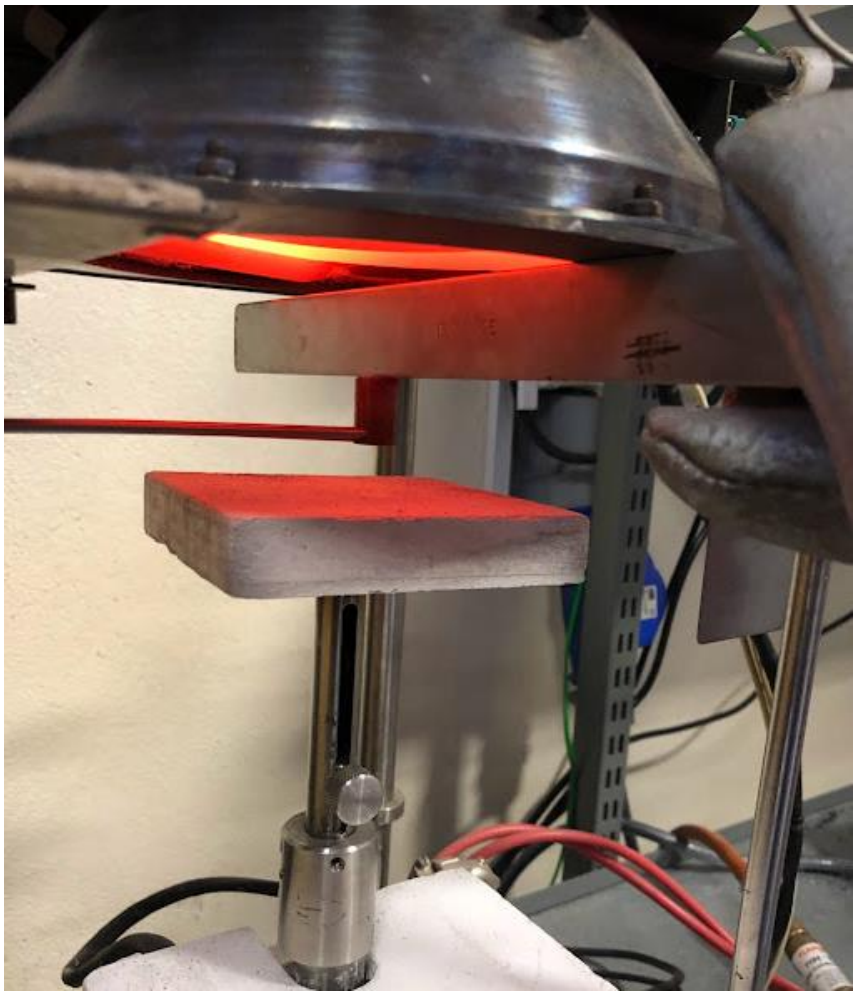

Figure 16: Flux meter positioning with a 25 mm ruler.

The HRR was checked with a methane flow rate corresponding to 3 kW as requires the standard [68]. If this reached a difference greater than 5%, the position of the thermopile had to be checked. When it was not a problem, the equipment needed to be recalibrated.

All these proceedings had to be done every time the operating heat flux was changed to.

3.4.6 TEST PROCEDURE

Then, once everything was set, the test was started following EN ISO 13927, [68], proceedings. By first, the power of the cone heater and the extractor fan were turned on. Then, it was needed to calibrate the equipment as previously explained in section 3.4.5 of this work.

To start the test, it was necessary, with the shield closed, first to place the sample holder with the right amount of ceramic fiber in the load cell and tare the set. Then this sample holder was removed and another empty one was put in its place. The shield was then opened and it

was needed to wait until the temperature stabilize again. While waiting, the sample could be placed in the holder with the ceramic fiber. Once the temperature of the cone was stable, it was necessary to collect the baseline with the sample holder empty for 60 seconds. Figure 17 shows the sample holder empty and positioned for the baseline collection. The empty sample holder placed on the top of the load cell was removed and then the test could get started.

Figure 17 (a and b): sample holder empty and positioned for the baseline collection, respectively.

Then, the sample was covered with gypsum board to protect its surface so that it suffers as little heat influence as possible before the actual start of the test, see Figure 18. Then, the specimen was positioned. The "Start Test" icon was selected in the software at the same time the gypsum board was taken out and the output data started to be collected. The spark plug was moved into place and its power was turned on. So it was lighting up continuously. As soon as the ignition occurred, I needed to press the "I" key on the keyboard so that the ignition time (Tign) was computed.

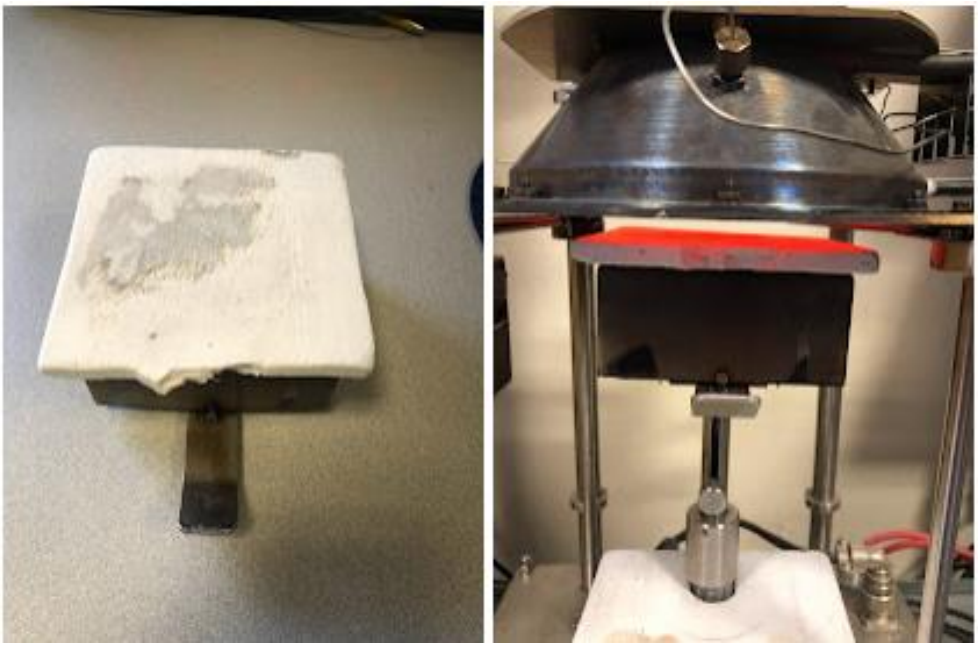

Figure 18: Sample covered with gypsum board to protect its surface before test.

Figure 19 shows the moment after ignition with the sample on fire. When the flame went out, the "F" key on the keyboard had to be pressed in order for the flameout time to be recorded. The test was ended when the mass value indicated by the load cell was stable.

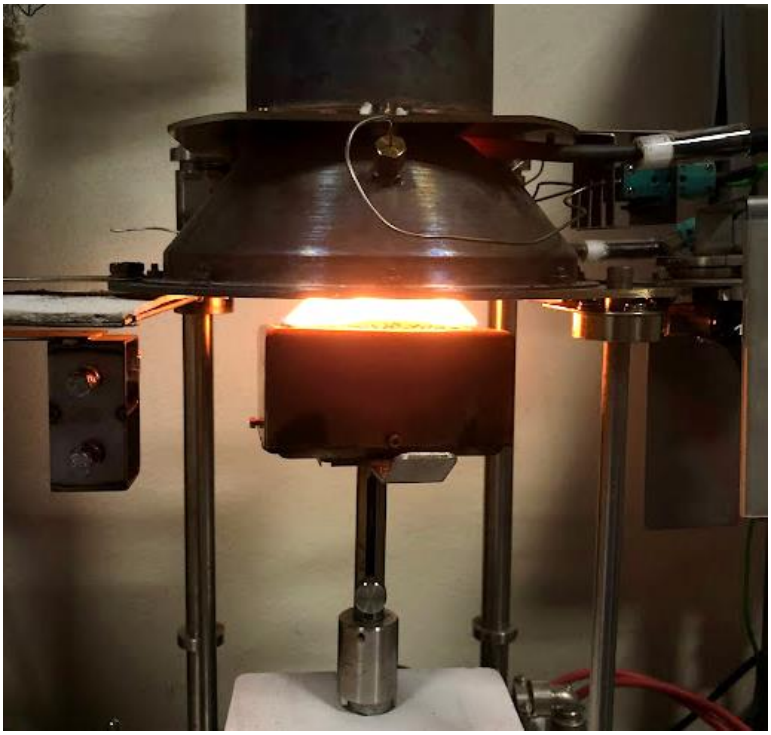

Figure 19: Specimen on fire during a test.

3.4.7 ADOPTED HEAT FLUX

In the analysis of reaction to fire, it is common to carry out tests for constant flow of 35, 50 and 75 kW. These flows simulate the stages of a fire. A flux of 35 kW/m² simulates the beginning of fire propagation, a flux of 50 kW/m² simulates the beginning of flashover and a flux of 75 kW/m² simulates a fully developed fire, [67].

The present work evaluates the thermal performance of a multilayer panel in which only its core varies. In this way, the beginning of fire propagation should not change, since it occurs in the external layer of the panel. Therefore, it only depends on the properties of the MDF, already tested before, [82]. With this in mind, it was determined that the heat fluxes that would be evaluated are 50 and 75 kW/m².

The standard, [68], determines that at least 3 tests per type must be performed for a more reliable analysis of the results.

Chapter 4: Results and Discussions

In this chapter, the main results obtained during the work will be presented. Both the production of cork agglomerates and the tests in the calorimetric cone for each of the compositions. The graphs with the junction of the results for each heat flux tested will be presented.

4.1 AGGLOMERATED CORK PANELS

4.1.1 SMALLER MOULD

4.1.1.1 Panels made from MDI

First, it was defined the parameters for the manufacture of agglomerates with MDI resin. Once all the parameters were defined, these values were tested in the fabrication of panels with TDI resin.

It was noted that the pressure of 2 MPa was too high for making the panels. The first test, shown in Figure 20, had a noticeably unsatisfactory result. The panel was completely deformed and it was assumed that this was due to the high pressure.

In addition, the amount of water to be added to the mixture was not stated in any of the articles read for the theoretical framework of this work. Therefore, initially a value of 35% of the total weight of cork and resin in water was chosen. It is worth remembering that the density of water is much greater than that of cork, so in terms of volume, it is a small amount.

However, it was noticed that during pressing, resin overflowed. In Figure 21 it is possible to see marks of resin that flowed on the base of the mould. Therefore, it was assumed that there was a lot of water. This factor is bad, because if there was a resin leak, it means that the agglomerate was left with less resin than expected, impairing the adhesion between the particles.

For the purposes of analysing the influence of each factor, it is important to change only one parameter at a time. Pressure was believed to have a greater influence on the unsatisfactory outcome than the amount of water. So, it was decided to test lower pressures. A new attempt was made at half the initial pressure. There was a visual improvement, but the panel was still

not satisfactory. The agglomerate was extremely compacted and presented a "swollen" region, as shown in Figure 22.

Figure 20: Panel faulty due to excessive pressure applied

Figure 21: Mould with traces of run-off resin.

Figure 22: Extremely compacted agglomerate with a rupture inside.

Then, tests were carried out with lower pressures and longer pressing times until the best solution was found: applying the minimum pressing force (6 kN), which means a pressure of around 220 kPa taking into account the area of this mould, during 2 hours and 15 minutes.

4.1.1.2 Panels made from TDI

Once all the parameters used for the agglomerates made with MDI resin were defined, they (except the temperature) were used for the manufacture of the panels with TDI.

However, although the MDI panels were successful, the TDI panels showed swelling in the middle even with longer pressing time. It was assumed that this factor was happening due to the different properties of the resins. While the MDI is more rigid, the TDI is more flexible. The pressure was probably too high for the TDI resin to maintain adhesion between the particles.

As the pressure used was already the minimum force of the machine used for pressing, it was then decided to test making TDI agglomerates in the larger mould, since a larger area distributes more force and, as a consequence, implies a lower pressure.

It was noticed that the TDI panels were softer and smoother to the touch than the MDI ones. Possibly also because this resin is more flexible.

4.1.2 LARGER MOULD

Once the parameters for manufacturing the panels on a small scale were defined, the manufacturing of larger agglomerates began.

It was decided to make panels with a lower density than those previously made on a smaller scale, for two reasons. First, it was seen that TDI, being more flexible than MDI, cannot hold a panel of that density and with that it would not be possible to compare the two resins. Second, considering the final product of the fire door, a very high density for the panel would imply a heavier door, which is not so advantageous.

The input settings of the press used were plate temperature, force to be applied and pressing time. Therefore, there was no way to set a desired thickness for the panel. Thus, it was sought to find a relationship between the force applied by the press and the final thickness of

the panel. For this, several different panels were produced with different amounts of cork-resin mixture and different pressing forces.

The density chosen for the panels was around 160 kg/m³, a density considered medium for agglomerated cork, [30]. The thicknesses chosen were 12 and 19 mm, because smaller thickness would not add much thermal resistance to the door and a greater thickness would imply a very wide door.

Once the panels were ready, they were marked so that they could be cut to a size of 100 x 100 mm, as required by the standard for testing in the calorimetric cone.

4.1.3 MATLAB CODE TO CALCULATE THE PARAMETERS NECESSARY FOR THE MANUFACTURE OF EACH PANEL

A spreadsheet was set up with data from 12 panels and a linear relationship between the applied pressure and the density of the panels was noted. Thus, with the help of the Origin software, [83], it was possible to estimate the equation of this relationship. A linear relationship between the parameters was noted. Therefore, a linear fitting was performed. The resulting equation and its associated error are described in the graph of shown in Figure 23.

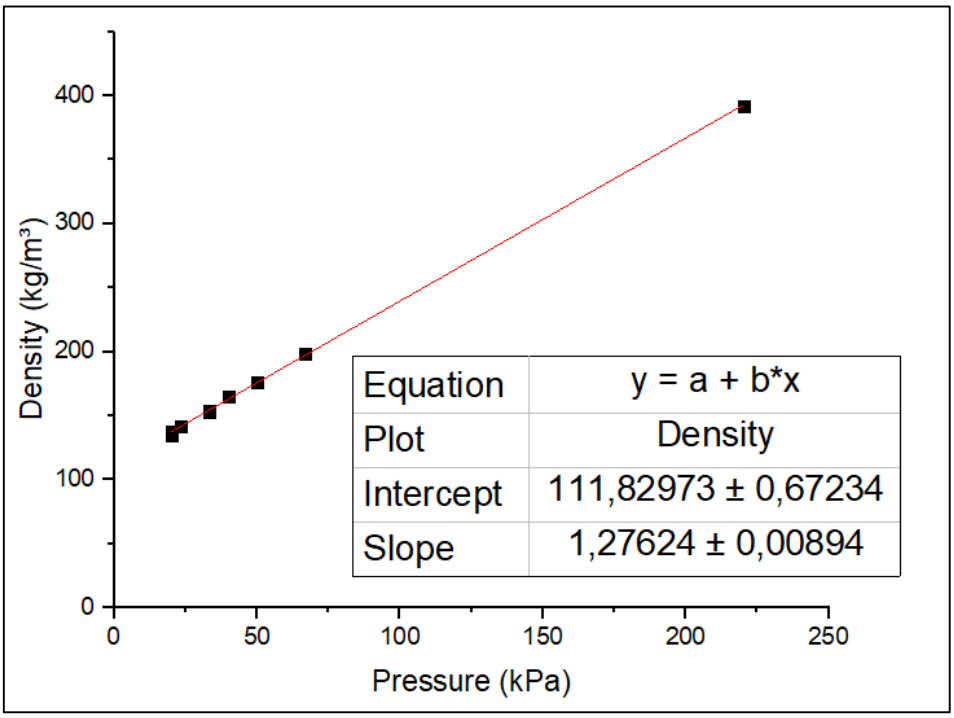

Figure 23: Graph of the relationship between the applied pressure and the final density of the panels.

For the MATLAB equation to encompass any amount of agglomerate mix, it was also necessary to plot the relationship between the compression ratio and the applied pressure, Figure 24. The compression ratio was based only on the volume of cork with larger granules.

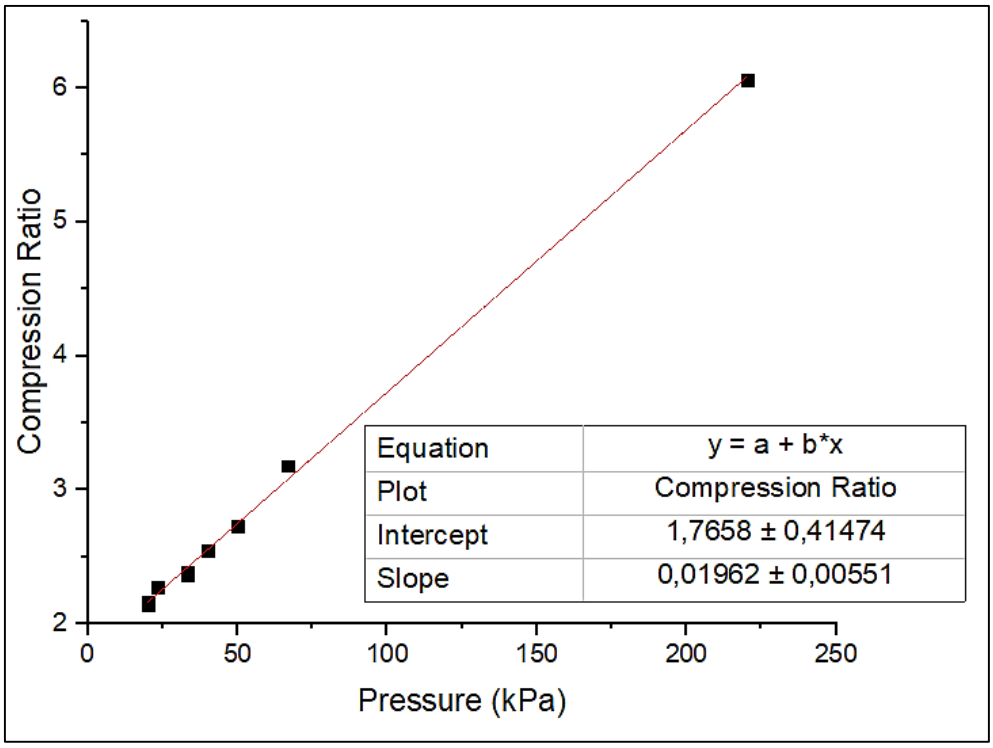

Figure 24: Graph of the relationship between the applied pressure and the compress ratio of the cork.

Then, these equations were passed to a code in the MATLAB software so that only with the inputs "final panel thickness", "density", and "mould base area" it was possible to know the amount of cork, resin and water, and which force is needed to manufacture that desired panel.

The code is described in Attachment I – MATLAB code to calculate the necessary parameters for the manufacture of each agglomerated cork panel.

With this code, it was possible to standardize the samples, including for continuations of this research and future works. In addition, the problem of not knowing the required strength and required amount of mix to manufacture a panel with the desired thickness and density has been resolved.

4.1.4 EXPANDABLE GRAPHITE

Adding the expandable graphite to the mix had difficulties in the beginning. By simply placing the graphite together with the cork and then adding the resin, it was noticed that a good part of the EG was at the bottom of the container and did not adhere very well to the mixture. Then, an attempt was made to pre-mix the graphite with the resin to ensure that all the combustible material (resin) was adhered to the flame retardant. However, the addition of this component caused the resin to become very thick. Thus, it was not possible to achieve a homogeneous mixture.

So, the best way found was to mix the panel normally, without the EG. And only after all the cork granules were covered with resin, gradually add the retardant. This addition was made by three-thirds. First add one third, mix, then another third and so on.

Figure 25, Figure 26 and Figure 27 show images taken with an optical camera at 200x optical zoom of cork panels with 0, 5, and 10% expanded graphite, respectively.

Figure 25: Agglomerated cork with 0% EG magnified at 200x.

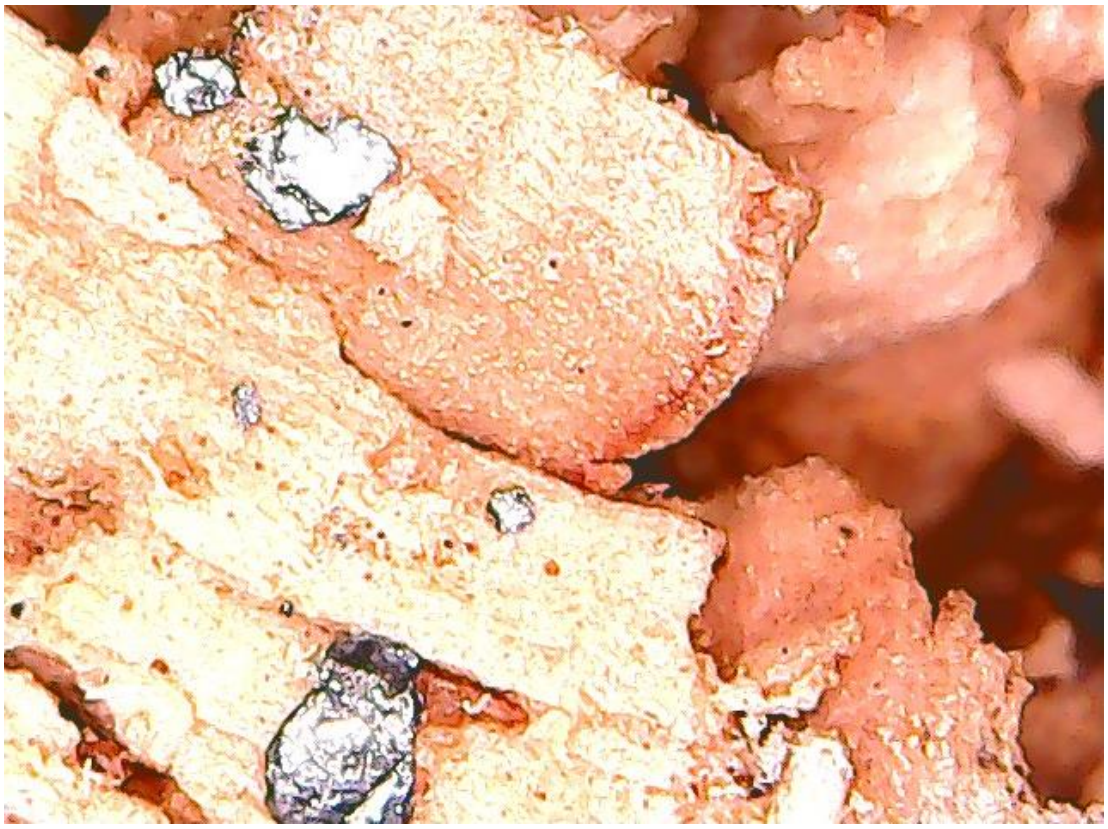

Figure 26: Agglomerated cork with 5% EG magnified at 200x.

Figure 27: Agglomerated cork with 10% EG magnified at 200x.

4.2 CONE CALORIMETER TEST

4.2.1 DETERMINATION OF THE USE OF SPECIMENS

Once the parameters of each sample were defined, it was possible to list the use of each sample. Table 3 includes the name of each sample, with the resin used in its manufacture, its thickness, the amount of expandable graphite added and the heat flux to which the sample was exposed during the test.

As previously defined in the experimental planning, in total there are two samples with 12 mm of thickness, one made with MDI and the other with TDI; and eight samples of 19 mm, with four different concentrations of EG (0%, 5%, 10% and 20%) for each type of evaluated resin.

Each sample was tested under two heat fluxes.

The table with the final composition of each panel is described in Attachment II – Table of panel mix component quantities.

Table 3: Composition and heat flux performed on each test piece.

Sample	Resin	Thickness (mm)	% of Expandable Graphite	Heat Flux (kW/m²)
TDI-12mm-0%EG-S1	TDI	12	0	75
TDI-12mm-0%EG-S2				
TDI-12mm-0%EG-S3				
TDI-12mm-0%EG-S4				50
TDI-12mm-0%EG-S5				
TDI-12mm-0%EG-S6				
MDI-12mm-0%EG-S1	MDI	12	0	75
MDI-12mm-0%EG-S2				
MDI-12mm-0%EG-S3				

MDI-12mm-0%EG-S4 MDI-12mm-0%EG-S5 MDI-12mm-0%EG-S6				50
TDI-19mm-0%EG-S1 TDI-19mm-0%EG-S2 TDI-19mm-0%EG-S3	TDI	19	0	75
TDI-19mm-0%EG-S4 TDI-19mm-0%EG-S5 TDI-19mm-0%EG-S6				50
MDI-19mm-0%EG-S1 MDI-19mm-0%EG-S2 MDI-19mm-0%EG-S3	MDI	19	0	75
MDI-19mm-0%EG-S4 MDI-19mm-0%EG-S5 MDI-19mm-0%EG-S6				50
TDI-19mm-5%EG-S1 TDI-19mm-5%EG-S2 TDI-19mm-5%EG-S3	TDI	19	5	75
TDI-19mm-5%EG-S4 TDI-19mm-5%EG-S5 TDI-19mm-5%EG-S6				50
MDI-19mm-5%EG-S1 MDI-19mm-5%EG-S2 MDI-19mm-5%EG-S3	MDI	19	5	75
MDI-19mm-5%EG-S4				50

MDI-19mm-5%EG-S5				
MDI-19mm-5%EG-S6				
TDI-19mm-10%EG-S1	TDI	19	10	75
TDI-19mm-10%EG-S2				
TDI-19mm-10%EG-S3				
TDI-19mm-10%EG-S4				50
TDI-19mm-10%EG-S5				
TDI-19mm-10%EG-S6				
MDI-19mm-10%EG-S1	MDI	19	10	75
MDI-19mm-10%EG-S2				
MDI-19mm-10%EG-S3				
MDI-19mm-10%EG-S4				50
MDI-19mm-10%EG-S5				
MDI-19mm-10%EG-S6				
TDI-19mm-20%EG-S1	TDI	19	20	75
TDI-19mm-20%EG-S2				
TDI-19mm-20%EG-S3				
TDI-19mm-20%EG-S4				50
TDI-19mm-20%EG-S5				
TDI-19mm-20%EG-S6				
MDI-19mm-20%EG-S1	TDI	19	20	75
MDI-19mm-20%EG-S2				
MDI-19mm-20%EG-S3				
MDI-19mm-20%EG-S4				50
MDI-19mm-20%EG-S5				

MDI-19mm-20%EG-S6				

4.2.2 RESULTS OF MASS LOSS

The values of mass loss of each sample were obtained through data acquisition from the software used. As the standard required that the tests be carried out in triplicate, an average of the values obtained for each composition was subsequently calculated. Then, to standardize the data to be analysed, the m/m0 ratio was calculated between the sample's mass during the test (m) and the initial value of the sample's mass (m0). These data were then processed and organized into graphs.

4.2.2.1 Samples without flame retardant

Figure 28 and Figure 29 show the graphs of mass loss throughout the test of agglomerates without flame retardant by heat flux tested.

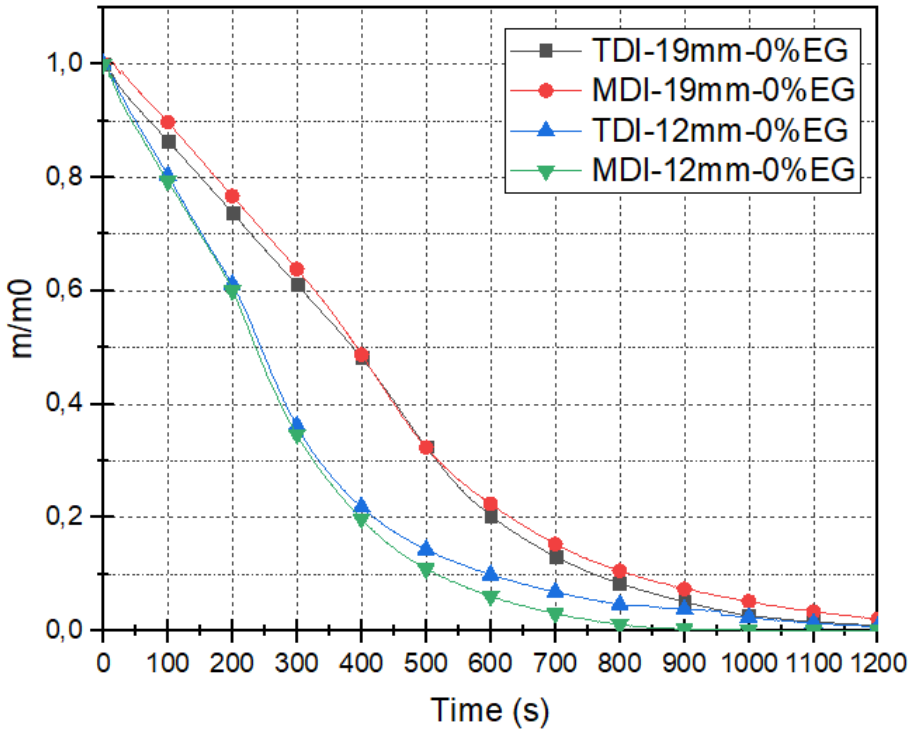

Figure 28: Graph of the mass loss of specimens without flame retardant tested for a heat flux of 50 kW/m².

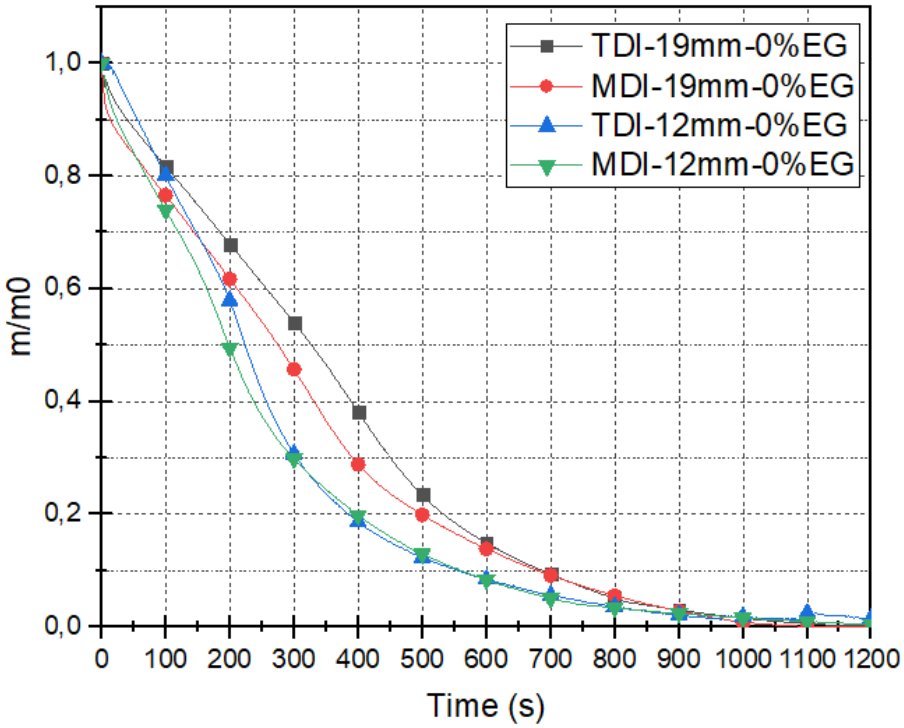

Figure 29: Graph of the mass loss of specimens without flame retardant tested for a heat flux of 75 kW/m².

The tests for the heat flux of 50 kW/m² showed that the way in which the specimen loses mass has more to do with its thickness than with the resin used. This is probably due to the fact that the resin mass is only 10% of the total mass of the sample. Therefore, its burning has little influence on mass loss.

For this heat flux value, there was a large difference between the composting of samples with different thicknesses. The 12 mm specimens lost half their mass about 150 seconds earlier than the 19 mm specimens. As for the samples tested at 75 kW/m², this time difference was a little smaller (around 100 seconds).

The flux of 75 kW/m² resulted in a faster mass decay. While the 19 mm samples lost 50% of their mass after approximately 400 seconds of running test at 50 kW/m2, for 75 kW/m² this time reduced to 330 seconds (TDI) and 280 seconds (MDI)

There was no residual mass in any of the cases. Figure 30 shows a specimen without EG after the end of the test.

Figure 30: A specimen without flame retardant after the end of the test.

4.2.2.2 Samples with Expandable Graphite

To evaluate the samples with expanded graphite adding, two graphs were plotted for each heat flux. Each of them presents samples of one type of resin, including the sample without EG for comparison purposes.

For the heat flux of 50 kW/m², tests were also carried out for samples with 20% of expandable graphite. However, these samples were not carried forward, because the EG, when it expands due to the heat, becomes very light and ends up being carried away by the air current that arises due to natural convection during the test. Thus, it is not possible to know what of the mass was lost due to convection and what was lost due to burning. Figure 31 shows how the test environment was after the tests performed with samples with 20% EG. Another problem that happened during the rehearsal of this sample was that as there was a lot of EG, it expanded too much and touched the cone, Figure 31**Erro! Fonte de referência não encontrada.**. In this way, it ended up making a contrary force and caused changes in the value of the mass read by the load cell during the test. This mainly happened with samples made with TDI. For these reasons, it was decided not to continue with samples with this composition.

Figure 31: Working environment after testing a TDI sample with 20% expandable graphite.

Figure 32: TDI sample with 20% expandable graphite touching the cone during a test.

TDI samples with 10% EG showed the same problem as those with higher concentration of the additive, but as the visual amount of expanded graphite flying during the test due to convection was low, it was decided to proceed with the samples.

Figure 33 and Figure 34 shows 200x optical zoom photos of pure expandable graphite before and after being exposed to heat, respectively. Note that it ceases to be in grains and takes on a filament format.

Figure 33: EG before being exposed to heat (200x zoom).

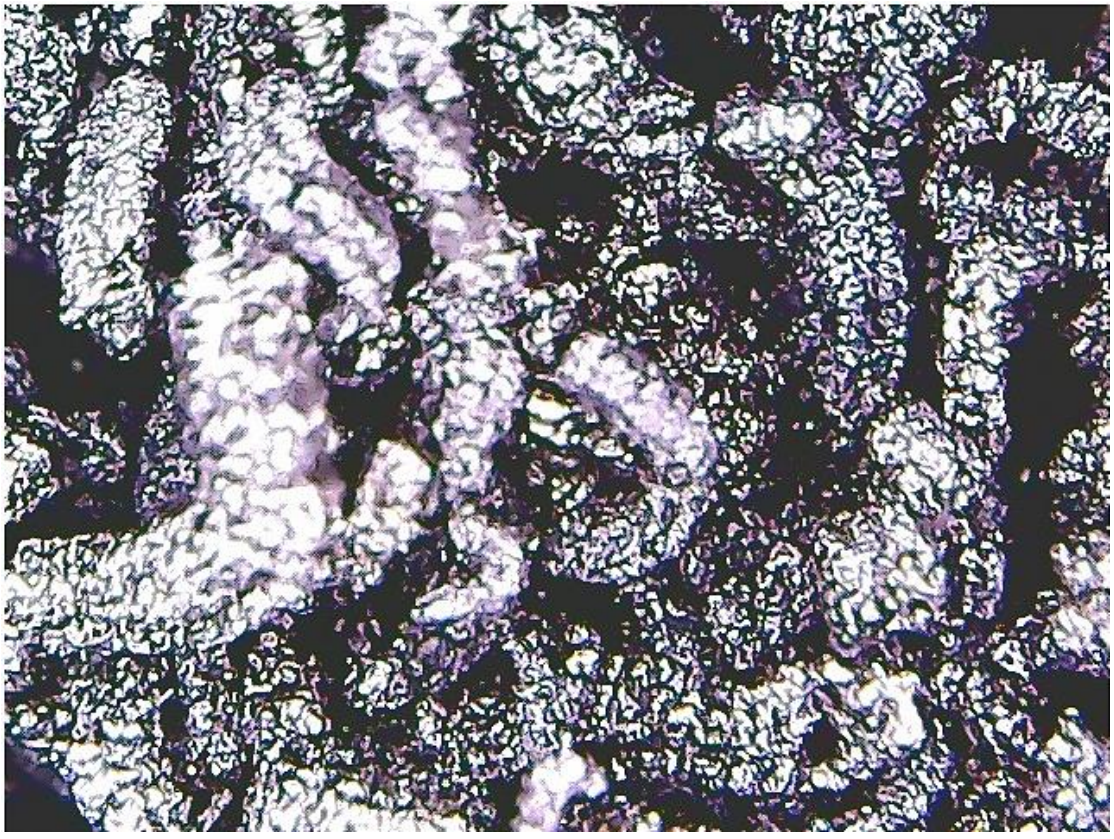

Figure 34: EG after being exposed to heat (200x zoom).

Figure 35 and Figure 36 show the mass loss graphs of MDI and TDI samples, respectively, with different EG concentrations for a flux of 50 kW/m². Figure 37 and Figure 38 show the graphs with the mass loss results of the same samples, but this time for tests carried out at 75 kW/m².

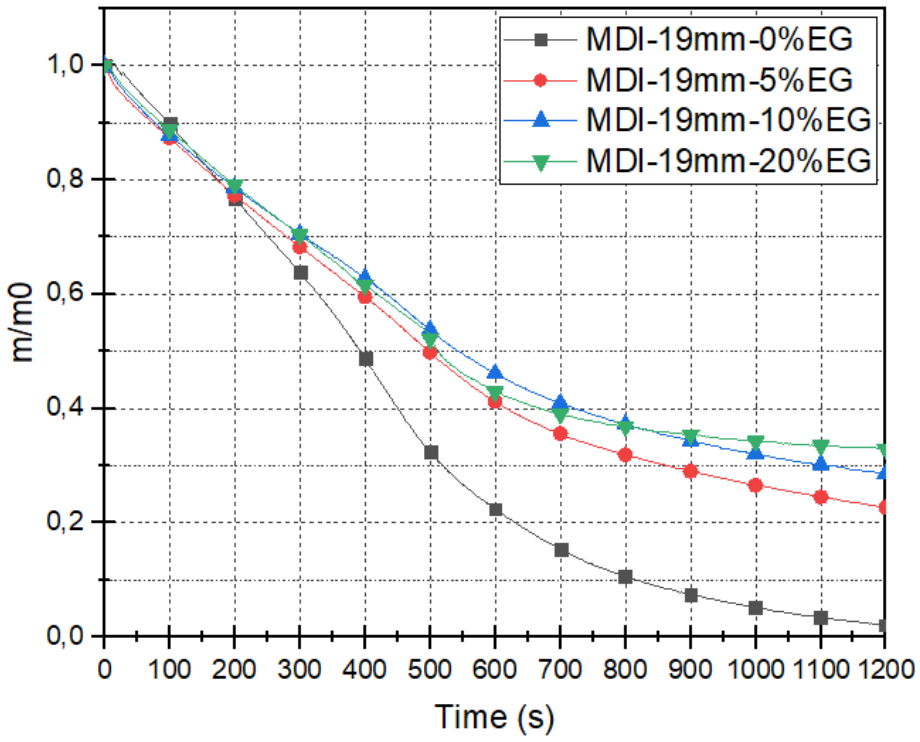

Figure 35: Mass loss graphs of MDI samples with different EG concentrations for a flux of 50 kW/m².

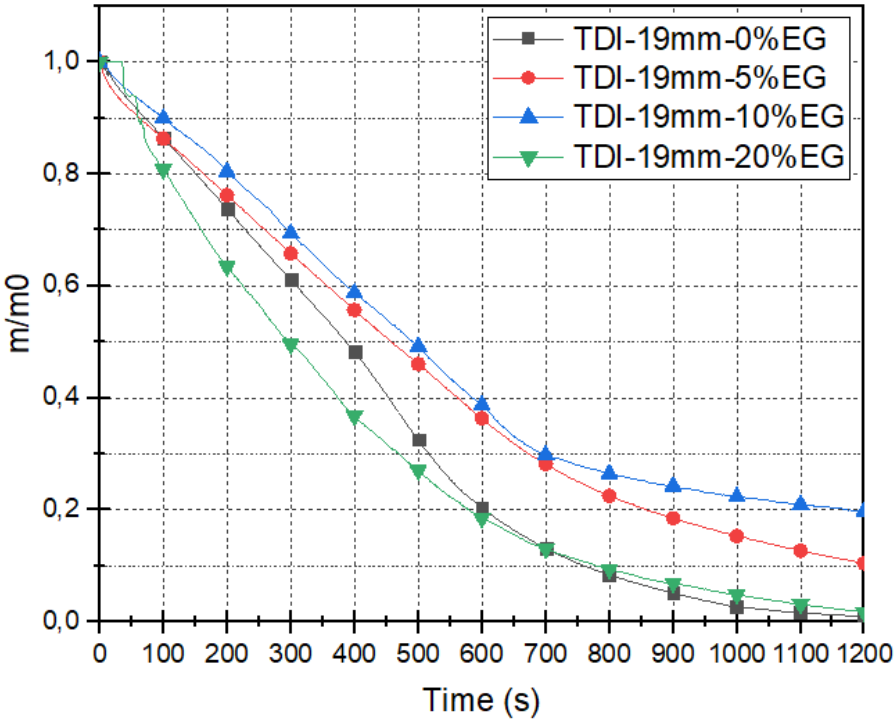

Figure 36: Mass loss graphs of TDI samples with different EG concentrations for a flux of 50 kW/m².

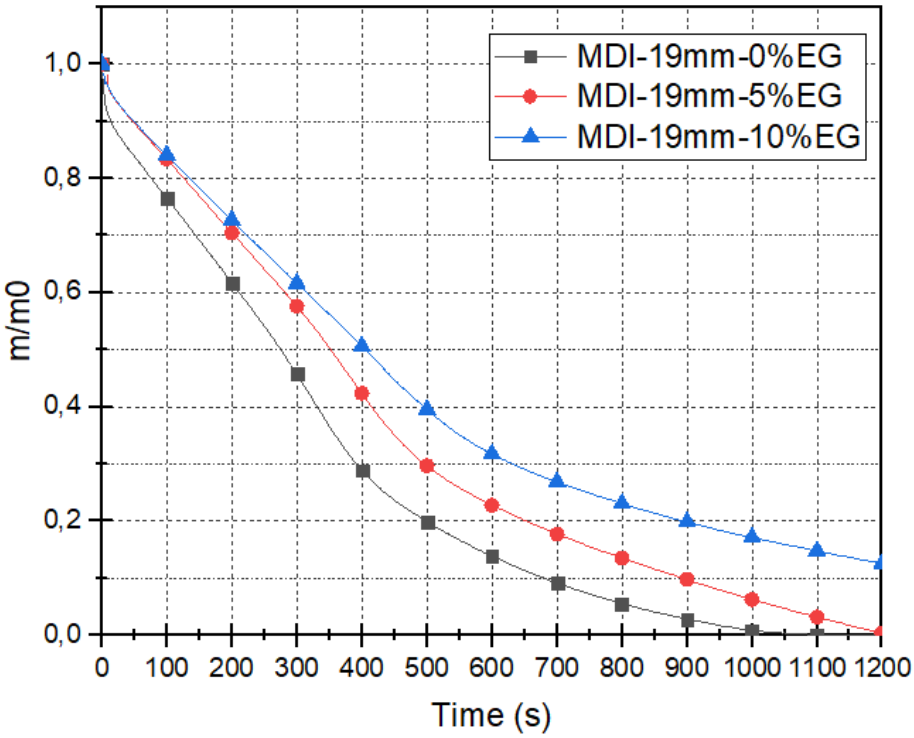

Figure 37: Mass loss graphs of MDI samples with different EG concentrations for a flux of 75 kW/m².

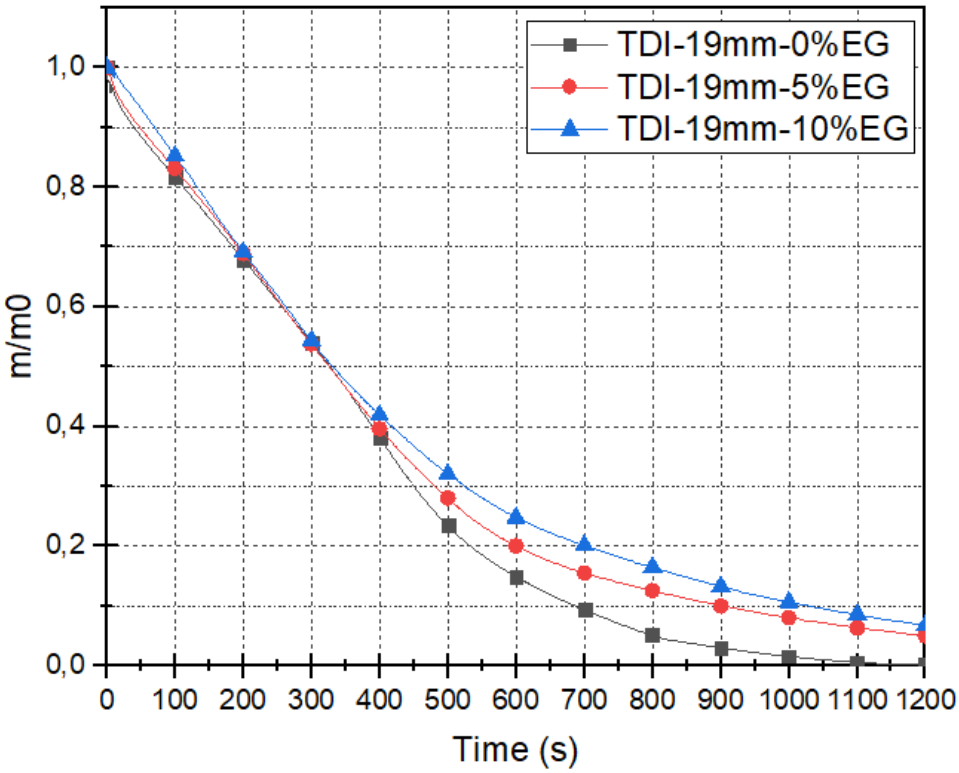

Figure 38: Mass loss graphs of TDI samples with different EG concentrations for a flux of 75 kW/m².

The addition of expandable graphite resulted in a slower mass loss, mainly in tests carried out at 50 kW/m².

Figure 36 shows that TDI samples with 20% EG did not present a satisfactory result. Its mass was lost very quickly during the test, when compared to the other samples. This is due to the fact that as it released a lot of large soot with natural convection during the test. Thus, it is not known how much mass was actually lost and the results, as a consequence, are not reliable. For these reasons, it was decided to discard samples with 20% of additive.

With the results obtained, it was possible to evaluate that, except in the exceptional cases described, there was a direct relationship between the amount of expandable graphite and the loss of mass. Specimens with higher concentrations of EG showed lower mass loss during the tests performed in both flows, regardless of the type of resin.

Figure 39 and Figure 40 show samples of MDI with 5 and 10%, respectively, of EG after a test carried out at 50 kW/m².

Figure 39: MDI specimen with 5% of EG after a test carried out at 50kW/m².

Figure 40: MDI specimen with 10% of EG after a test carried out at 50kW/m².

4.2.3 RESULTS OF HEAT RELEASE RATE (HRR) AND TOTAL HEAT RELEASED (THR)

The values of Heat Release Rate (HRR) and Total Heat Released (TRH) of each sample were obtained through data acquisition from the software used. An average of the values obtained for each composition was calculated. The software also displays the peak of the HRR. These data were then processed and organized into graphs and tables so that the results of all 48 tests could be analysed.

4.2.3.1 Samples without flame-retardant

In Figure 41 and Figure 42, it is possible to observe the averages of the heat release rate results of pure agglomerate samples with 12 and 19 mm thickness for the heat fluxes of 50 and 75 kW/m², respectively.

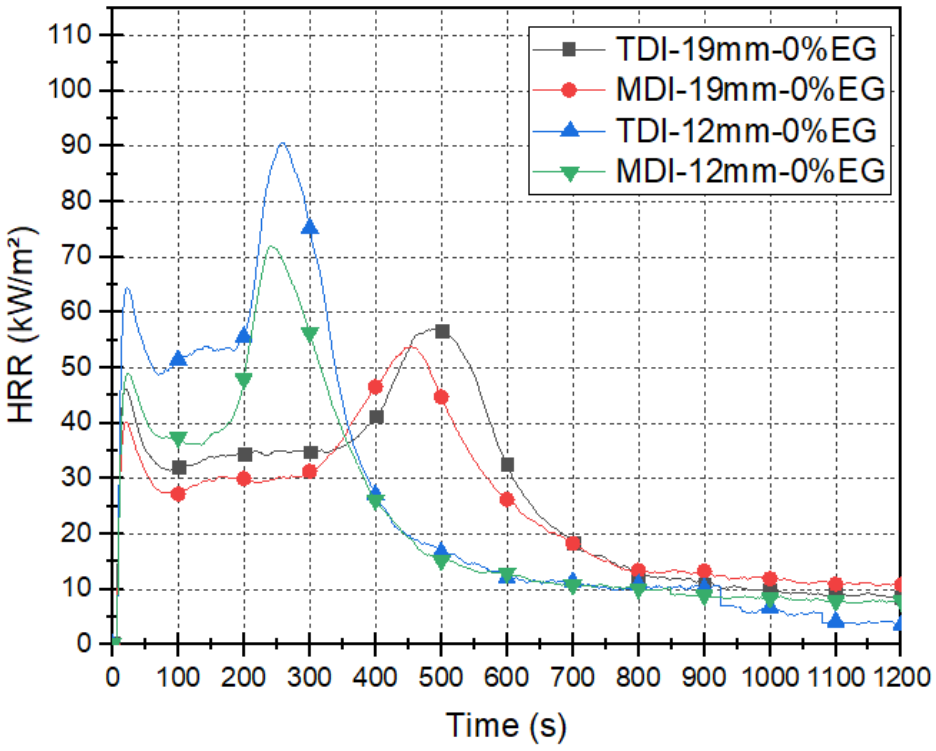

Figure 41: Graph of the averages of Heat Release Rate (HRR) of samples without EG at a heat flux of 50 kW/m².

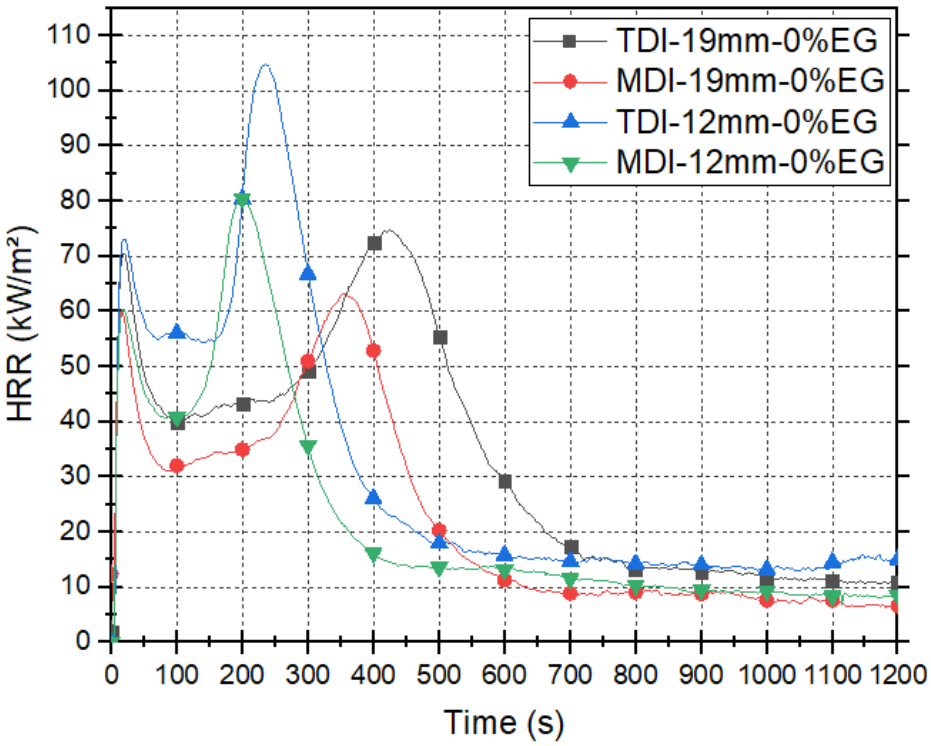

Figure 42: Graph of the averages of Heat Release Rate (HRR) of samples without EG at a heat flux of 75 kW/m².

To facilitate the comparison, Table 4 and Table 5 describe the peak values and the time at which they occurred in the tests for the fluxes of 50 and 75 kW/m², respectively.

Table 4: HRRpeaks of samples without EG tested at 50 kW/m².

Sample	**HRRpeak1 (kW/m²)**	**Time HRRpeak1 (s)**	**HRRpeak2 (kW/m²)**	**Time HRRpeak2 (s)**
TDI-19mm-0%EC	46.2	20	56.9	492
MDI-19mm-0%EC	40.2	21	53.9	452
TDI-12mm-0%EC	64.4	22	90.7	260
MDI-12mm-0%EC	48.9	25	72.0	241

Table 5: HRR peaks of samples without EG tested at 75 kW/m².

Sample	HRRpeak1 (kW/m²)	Time HRRpeak1 (s)	HRRpeak2 (kW/m²)	Time HRRpeak2 (s)
TDI-19mm-0%EG	70.6	19	74.8	425
MDI-19mm-0%EG	60.3	16	63.3	355
TDI-12mm-0%EG	73.2	19	104.8	232
MDI-12mm-0%EG	60.4	18	80.5	201

Both heat fluxes showed similar results. All samples had two HRR peaks. The first peak was at the very beginning of the trial for all four cases, when the ignition happened.

It was also possible to see that for the same thickness, the samples made with TDI had higher HRR peaks than the MDI panels. Therefore, the MDI resin presents a lower risk of fire.

Thinner agglomerates had the second peak earlier than the thicker ones. Which means that, in a fire situation, there would be less time before the material becomes engulfed in flames. These samples also showed higher HRR for both fluxes tested. In other words, in addition to the peak happening earlier, it is also more intense, which would be disadvantageous.

After the second peak, the 12 mm specimens had a marked decrease in the rate of heat release. This is due to the fact that a large part of its mass had already been consumed and at this point in the test there was little combustible material left.

In Figure 43 and Figure 44, it is possible to observe the averages of the results of the total heat released from the samples without EG for the heat fluxes of 50 and 75 kW/m², respectively.

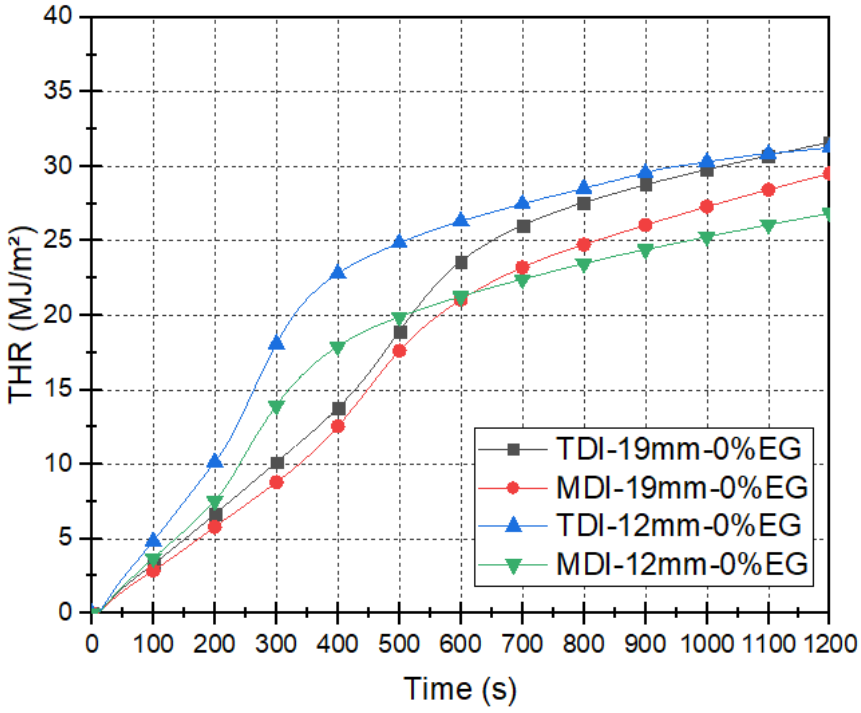

Figure 43: Graph of the averages of Total Heat Release (THR) of samples without at a heat flux of 50 kW/m².

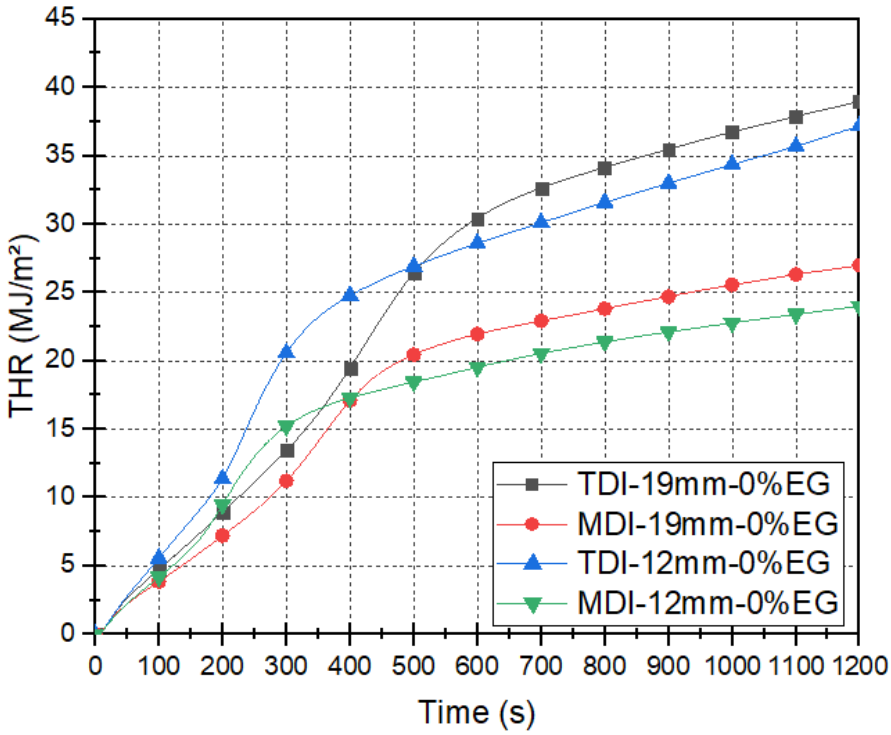

Figure 44: Graph of the averages of Total Heat Release (THR) of samples without at a heat flux of 75 kW/m².

Table 6 and Table 7 present the average of value of Total Heat Released (THR) recorded for the pure agglomerates for each tested flux after 1200 seconds.

Table 6: THR after 1200 seconds of tests performed on pure samples at 50 kW/m².

Sample	**THR(1200) (MJ/m²)**
TDI-19mm-0%EG	31.6
MDI-19mm-0%EG	29.5
TDI-12mm-0%EG	31.3
MDI-12mm-0%EG	26.9

Table 7: THR after 1200 seconds of tests performed on pure samples at 75 kW/m².

Sample	**THR(1200) (MJ/m²)**
TDI-19mm-0%EG	39.0
MDI-19mm-0%EG	27.0
TDI-12mm-0%EG	37.2
MDI-12mm-0%EG	24.0

After analysing the graphs and tables, it was observed that even the TDI samples showing higher HRR peaks, the 50 kW/m² flux did not result in a large difference in THR, while the 75 kW/m² flux had a more significant difference between the MDI and TDI samples. But still, both TDI samples released more heat in total than MDI, regardless of thickness.

Although the HRR peaks of samples made with MDI are smaller, their curves are less sharp and remain high for longer. In this way, the difference between the peaks is compensated and the total heat released does not undergo much change in relation to the resins, only in relation to the thickness of the sample tested.

This comparison was made for 1200 seconds of running test. The 19 mm samples took longer to reach complete combustion and, as a consequence, if the total test time is analysed, they released more heat.

4.2.3.2 Samples with Expandable Graphite

Figure 45 and Figure 46 show the averages of the heat release rate results of MDI and TDI agglomerate samples, respectively, for the heat fluxes of 50, and Figure 47 and Figure 48 for 75 kW/m², respectively.

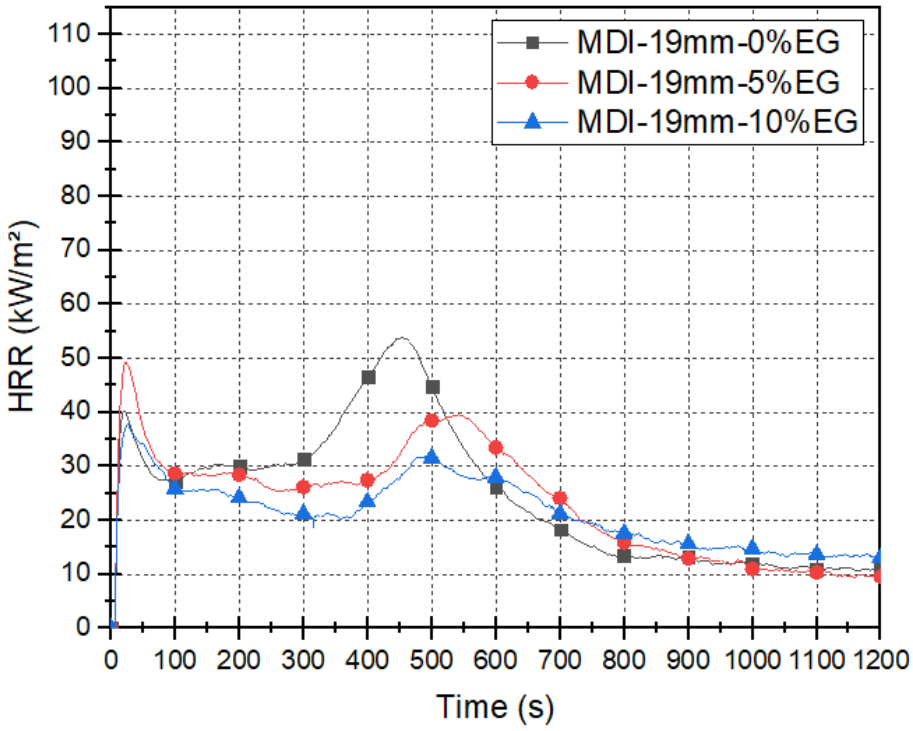

Figure 45: Graph of the averages of Heat Release Rate (HRR) of MDI samples with different concentrations of EG for a heat flux of 50 kW/m².

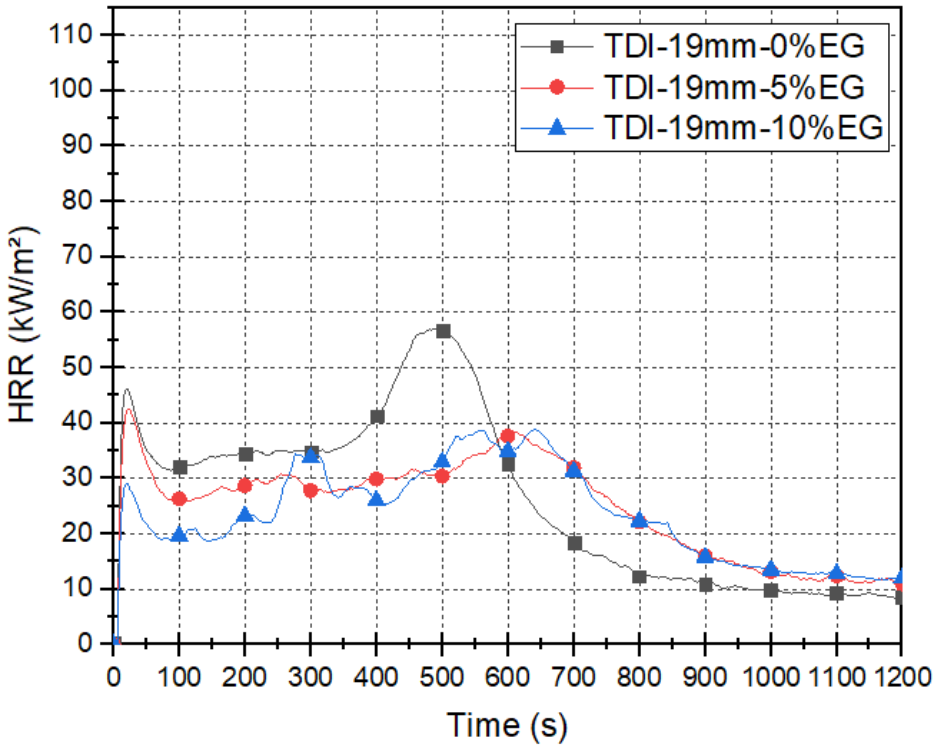

Figure 46: Graph of the averages of Heat Release Rate (HRR) of TDI samples with different concentrations of EG for a heat flux of 50 kW/m².

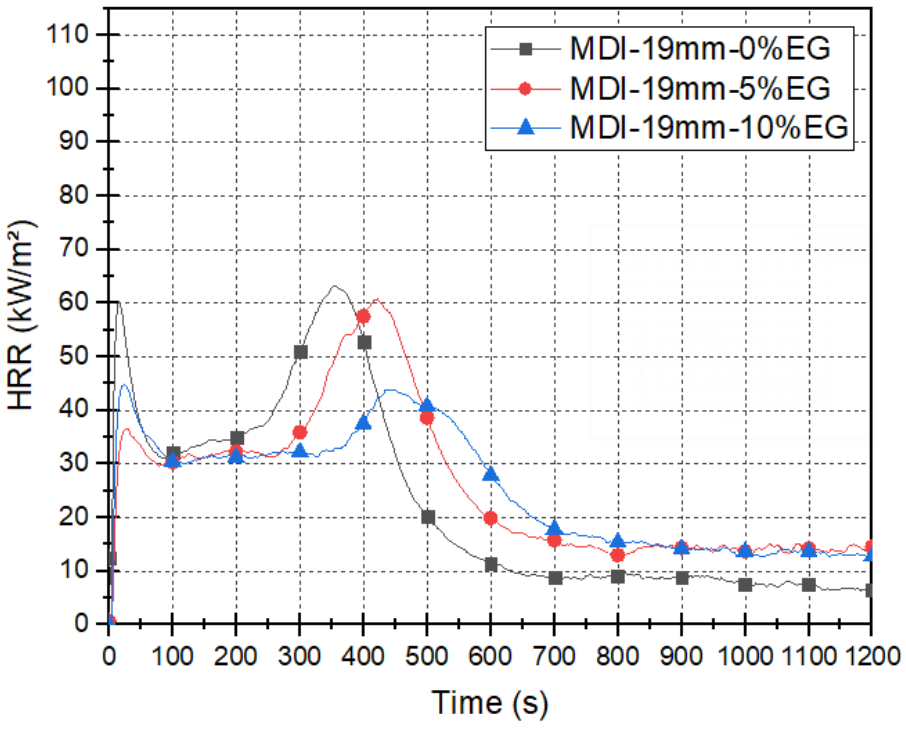

Figure 47: Graph of the averages of Heat Release Rate (HRR) of MDI samples with different concentrations of EG for a heat flux of 75kW/m².

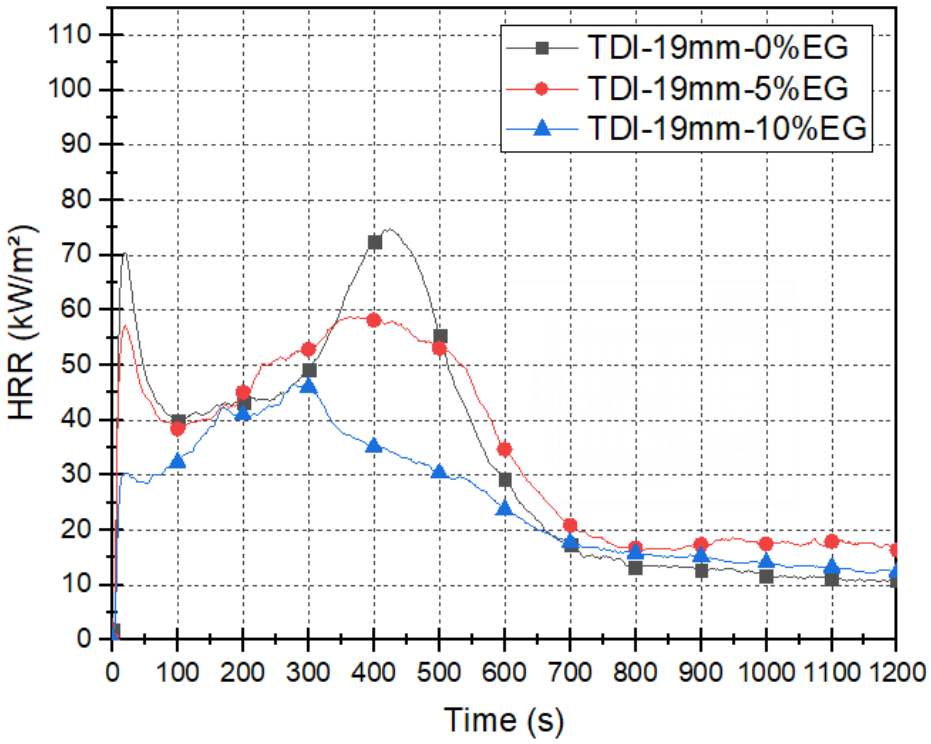

Figure 48: Graph of the averages of Heat Release Rate (HRR) of TDI samples with different concentrations of EG for a heat flux of 75 kW/m².

Table 8 and Table 9 describe the peak values and the time at which they occurred in the tests for the fluxes of 50 and 75 kW/m², respectively.

Table 8: HRRpeaks of samples with EG tested at 50 kW/m².

Sample	**HRRpeak1 (kW/m²)**	**Time HRRpeak1 (s)**	**HRRpeak2 (kW/m²)**	**Time HRRpeak2 (s)**
TDI-19mm-0%EC	46.2	20	56.9	492
MDI-19mm-0%EC	40.2	21	53.9	452
TDI-19mm-5%EC	42.6	23	38.3	613
MDI-19mm-5%EC	49.3	23	39.5	541
TDI-19mm-10%EC	29.1	20	38.8	639
MDI-19mm-10%EC	37.8	27	32.0	494

Table 9: HRR peaks of samples with EG tested at 75 kW/m².

Sample	HRRpeak1 (kW/m²)	Time HRRpeak1 (s)	HRRpeak2 (kW/m²)	Time HRRpeak2 (s)
TDI-19mm-0%EC	70.6	19	74.8	425
MDI-19mm-0%EC	60.3	16	63.3	355
TDI-19mm-5%EC	57.2	20	58.9	376
MDI-19mm-5%EC	36.6	27	60.8	422
TDI-19mm-10%EC	34.3	120	46.6	279
MDI-19mm-10%EC	44.7	25	43.9	437

It is noticeable that the addition of expandable graphite to the sample reduces the heat release during the test. In other words, it reduces the risk of fire.

MDI samples showed to react better with EG than TDI samples. They had resulted regular curves. The behaviour of the samples with the flame retardant is similar to that of the pure sample, but to a lesser extent.

But for samples made with TDI, this patterning of the heat release behaviour during the tests is not noticed. This is probably due to the reaction of the TDI with the EG releasing soot in blocks during combustion. As during the test, the soot of these samples was released in blocks, the release of heat was not uniform, as a result of which the loss of combustible material was not uniform.

Figure 49 and Figure 50 show the averages of the heat release rate results of MDI and TDI agglomerate samples, respectively, for the heat fluxes of 50, and Figure 51 and Figure 52 for 75 kW/m², respectively.

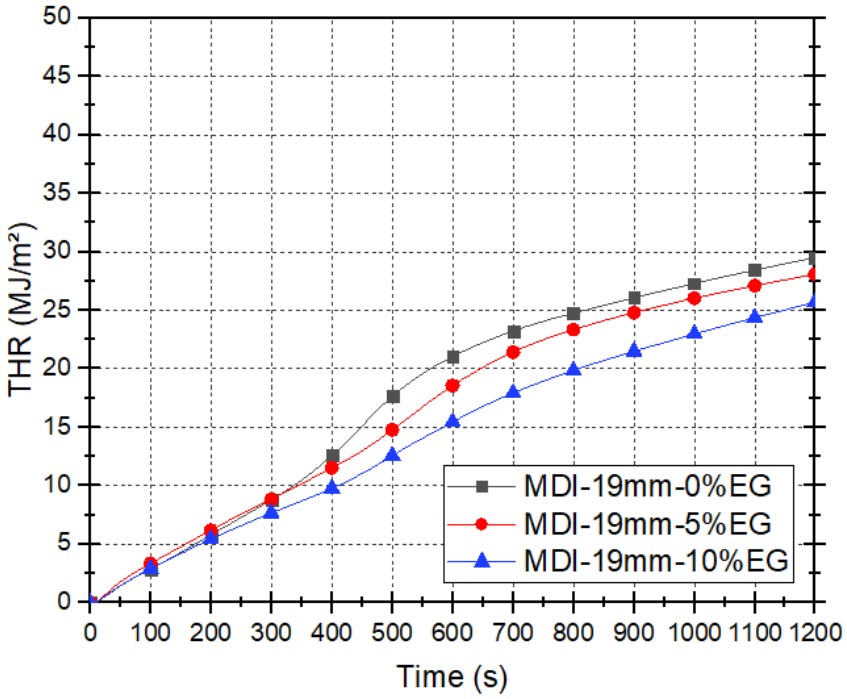

Figure 49: Graph of the averages of Total Heat Release (THR) of MDI samples with different concentrations of EG for a heat flux of 50 kW/m².

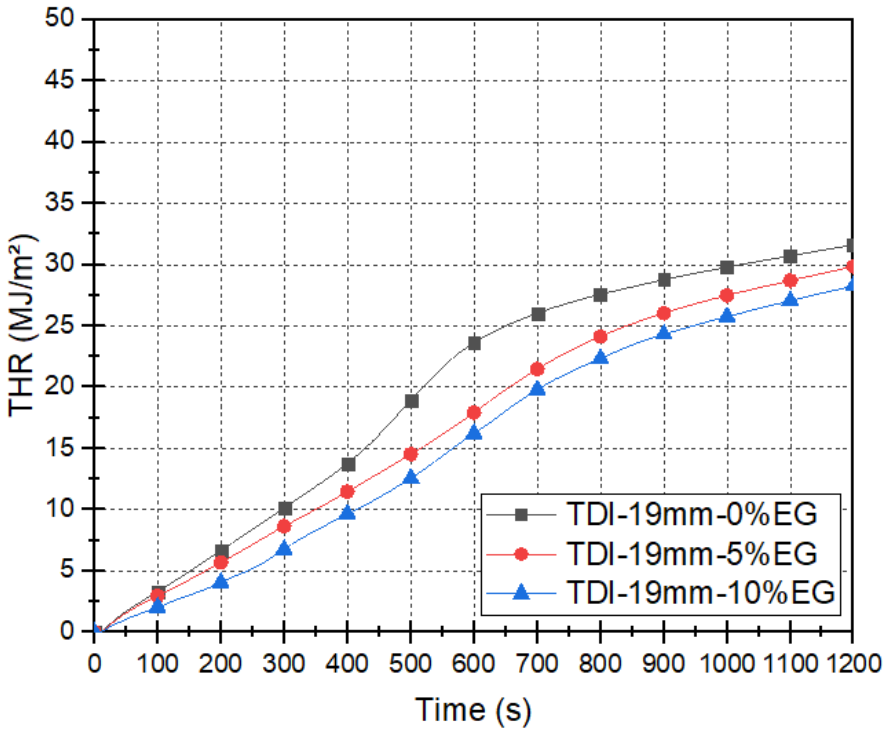

Figure 50: Graph of the averages of Total Heat Release (THR) of TDI samples with different concentrations of EG for a heat flux of 50 kW/m².

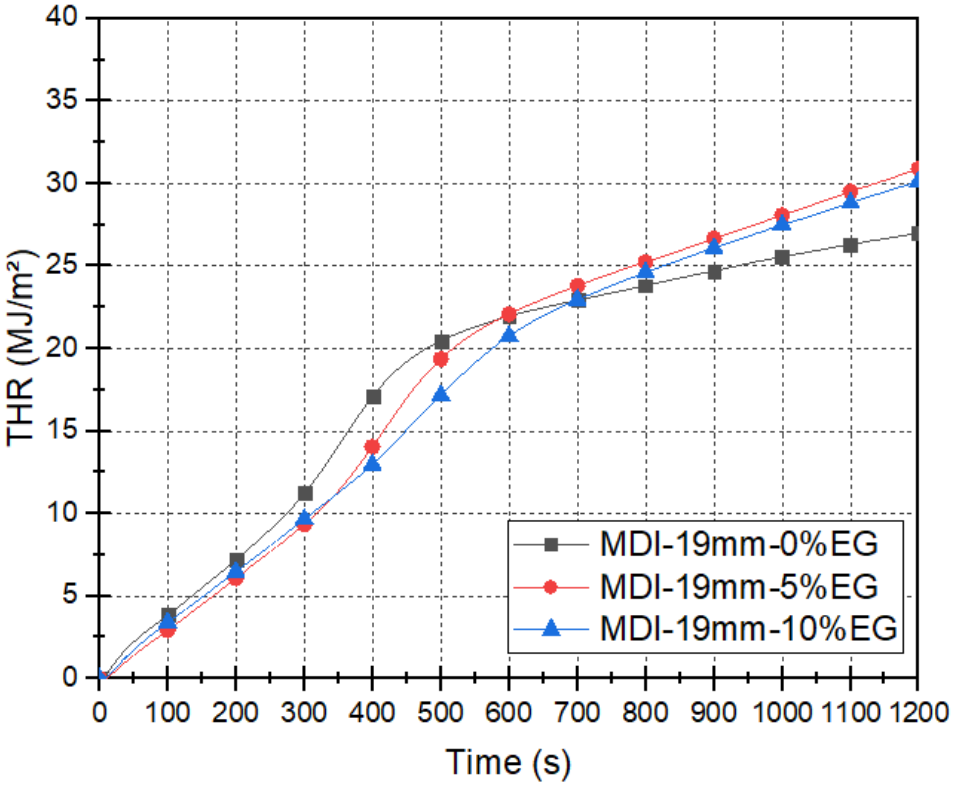

Figure 51: Graph of the averages of Total Heat Release (THR) of MDI samples with different concentrations of EG for a heat flux of 75kW/m².

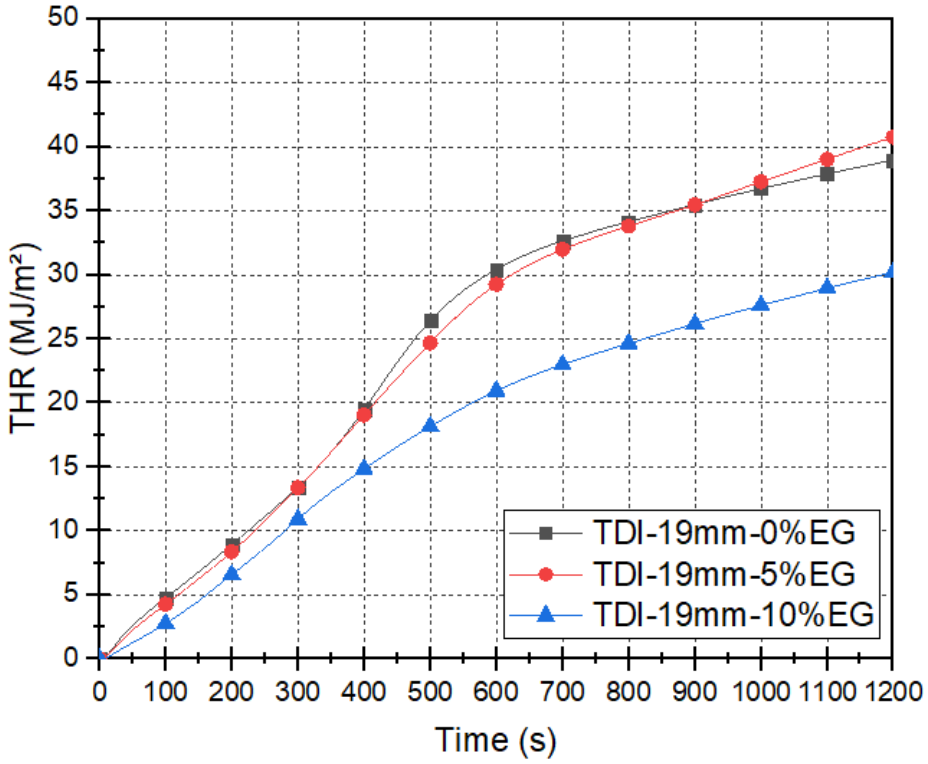

Figure 52: Graph of the averages of Total Heat Release (THR) of TDI samples with different concentrations of EG for a heat flux of 75 kW/m².

Table 10 and Table 11 present the average of value of Total Heat Released (THR) recorded for the samples with different concentrations of EG for each tested flux after 1200 seconds.

Table 10: THR after 1200 seconds of tests performed on samples with different concentrations of EG at 50 kW/m².

Sample	**THR(1200) (MJ/m²)**
TDI-19mm-0%EC	31.6
MDI-19mm-0%EC	29.5
TDI-19mm-5%EC	29.9
MDI-19mm-5%EC	25.7
TDI-19mm-10%EC	28.3
MDI-19mm-10%EC	25.7

Table 11: THR after 1200 seconds of tests performed on samples with different concentrations of EG at 75 kW/m².

Sample	**THR(1200) (MJ/m²)**
TDI-19mm-0%EC	39.0
MDI-19mm-0%EC	27.0
TDI-19mm-5%EC	40.8
MDI-19mm-5%EC	30.9
TDI-19mm-10%EC	30.2
MDI-19mm-10%EC	30.1

Tests performed at 50 kW/m² showed lower THR values for samples with EG. But although the addition of EG resulted in lower HRR peaks, in the sum, THR did not improve in tests performed at 75 kW/m².

There were no large variations between THR values. All were between 25 and 32 MJ/m² (with the exception of the TDI samples with 0 and 5% and EG tested at 75 kW/m²).

Chapter 5: Conclusion

5.1 GENERAL CONCLUSIONS

This work proposed to manufacture and analyse the fire behaviour of cork panels for use as the core of a wooden fire door through the test method recommended in the EN ISO 13927 standard, using the Cone Calorimeter equipment.

It was possible to make the panels and develop an equation to know how much mixture to put and how much force to apply in the press to produce a panel with the desired characteristics. The entire step by step was described in the work.

The methodology of the mass loss test was described, along with the equipment used and the results obtained for each of the tests performed. All tests obtained results of Heat Release Rate (HRR), mean HRR (MHRR), peak HRR (HRRpeak), and Total Heat Released (THR).

With this, it was possible to conclude during the realization of this thesis that regarding thickness, thinner samples, although they have less combustible material, show higher risk of fire than the thicker ones.

About the influence of the resin, MDI resin performs better on fire than the TDI resin. They had lower HRR and THR results than those made with the other resin. Although it has been noticed that the type of resin does not interfere much with the loss of mass.

However, an important factor to remember is that although the MDI specimens showed much lower peak values of HRR when compared to samples with the same concentration of EG made of TDI, the THR didn’t present such discrepant values.

Regarding the expandable graphite, it is concluded that it contributes significantly to the improvement of the panels' reaction to fire. However, it seems to react in an undesired way to TDI. There was a clear change in behaviour between the two resins.

5.2 SUGGESTIONS FOR FUTURE WORKS

Furthermore, still with the intention of studying the thermal performance, it is interesting to analyse the thermal properties such as conductivity and thermal diffusivity of the panels.

Another interesting study would be the chemical reaction between TDI resin and expandable graphite.

Then, still focusing on the development of a wood-based fire door, it is suggested that in future works the cork agglomerate studied in this work be applied as a core in a multilayer panel. It is recommended to use MDF as an outer layer.

It is good practice to test the cone calorimeter with the new composition. This time also for the constant flow of 35 kW/m². In addition, the author of this work suggests that tests be carried out on a medium scale according to EN 1363-1 [84] so the set can be classified according to EN 13501[16].

References

[1] EuroFSA, "Our Focus," *EU-Wide data on residential fires*, 2021. https://www.europeanfiresafetyalliance.org/our-focus/statistics/ (accessed Dec. 19, 2021).

[2] Directorate-General for Research and Innovation, *A sustainable Bioeconomy for Europe: Strengthening the connection between economy, society and the environment*. Brussels, Belgium, 2018.

[3] S. J. Davis *et al.*, "Net-zero emissions energy systems," *Science*, vol. 360, no. 6396, Jun. 29, 2018.

[4] DGAE, "Indústrias da Madeira e da Cortiça - Divisão 16 da CAE Rev. 3, excluindo subclasses 16293 a 16295 - Indústria da madeira e suas obras, exceto mobiliário; fabricação de cestaria e espartaria," Portugal, 2019.

[5] R. Jonsson *et al.*, "Boosting the EU forest-based bioeconomy: Market, climate, and employment impacts," *Technol. Forecast. Soc. Change*, vol. 163, p. 120478, Feb. 2021, doi: 10.1016/j.techfore.2020.120478.

[6] S. Kozlica and S. Dzidic, "Analysis of fire resistance of RC beams according to Eurocode 2," *MASE - Maced. Assoc. Struct. Eng.*, no. October, pp. 891–902, 2019.

[7] C. N. Costa, "Dimensionamento de elementos de concreto armado em situação de incêndio," Universidade de São Paulo, 2008.

[8] V. P. e Silva, "Estruturas de Aço em Situação de Incêndio," Universidade de São Paulo, 1997.

[9] T. Scheviak, "What are the Different Stages of a Fire?," 2021. https://www.firetrace.com/fire-protection-blog/different-stages-of-a-fire (accessed Feb.

05, 2022).

[10] P. Helene, C. Britez, and M. Carvalho, "Ações e efeitos deletérios do fogo em estruturas de concreto. Uma breve revisão," *Rev. ALCONPAT*, vol. 10, no. 1, pp. 1–21, Dec. 2020, doi: 10.21041/ra.v10i1.421.

[11] R. Ono, "Arquitetura de museus e segurança contra incêndios," *Semin. Int. NUTAU - An. em CD ROM*, 2004, [Online]. Available: https://repositorio.usp.br/item/001401877.

[12] EuroFSA, "Our Focus," *The growing vulnerable community*, 2021. https://www.europeanfiresafetyalliance.org/our-focus/the-growing-vulnerable-community/ (accessed Dec. 19, 2021).

[13] C. N. Costa, R. Ono, and V. P. e Silva, "A importância da compartimentação e suas implicações no dimensionamento das estruturas de concreto para situação de incêndio," in *Anais do 47º Congresso Brasileiro do Concreto - C3C2005*, 2005, no. Volume III-Efeito do Fogo em Estruturas de Concreto, pp. III1-26.

[14] APSEI, "Portas Resistentes ao Fogo," 2021. https://www.apsei.org.pt/areas-de-atuacao/seguranca-contra-incendio/portas-resistentes-ao-fogo/ (accessed Jun. 07, 2021).

[15] E. B. Ravinder and H. Nicmar, "Fire Door Awareness Among The Stake Holders Of Construction Industry," *Int. J. Appl. or Innov. Eng. Manag.*, vol. 9, no. 6, pp. 63–68, 2020.

[16] CEN, "EN 13501-2:2007+A1:2009 Fire classification of construction products and building elements —," *Eur. Comm. Stand.*, 2009.

[17] CEN, "EN1991-1-2:2002 (E) - Eurocode 1: Actions on structures - Part 1-2: General actions - Actions on structures exposed to fire -," *Eur. Comm. Stand.*, 2002.

[18] A. C. Pertile, "Análise numérica de vigas de madeira laminada colada reforçadas em situação de incêndio," Universidade Federal de Santa Catarina, 2018.

[19] A. J. Panshin and C. Zeeuw, *Textbook Of Wood Technology Vol I*, 3rd ed. New York: Mcgraw-Hill, 1970.

[20] P. Su, *Sorption of Metal Ions to Wood, Pulp and Bark Materials*. Painosalama Oy – Turku, Finland: Åbo Akademi University, 2012.

[21] M. M. L. dos Santos, A. C. P. da Cruz, I. C. de C. Terra, and C. O. V. R. Pereira, "Revisão integrativa do uso da madeira através do sistema construtivo wood frame no Brasil," *Res. Soc. Dev.*, vol. 11, no. 1, p. 9, Jan. 2022, doi: 10.33448/rsd-v11i1.24831.

[22] A. Amiri, J. Ottelin, J. Sorvari, and S. Junnila, "Cities as carbon sinks—classification of wooden buildings," *Environ. Res. Lett.*, vol. 15, no. 9, p. 094076, Sep. 2020, doi: 10.1088/1748-9326/aba134.

[23] E. I. Akpan, B. Wetzel, and K. Friedrich, "Eco-friendly and sustainable processing of wood-based materials," *Green Chem.*, vol. 23, no. 6, pp. 2198–2232, 2021, doi: 10.1039/D0GC04430J.

[24] F. Arouca, "Madeira na construção civil," *REMADE: Revista da Madeira*, p. 7, 2003.

[25] H. J. B. de Araujo, "Caracterização do material madeira," *Educ. Ambient. - o Desenvolv. Sustentável na Econ. Glob.*, pp. 31–44, 2020, [Online]. Available: http://www.alice.cnptia.embrapa.br/alice/handle/doc/1120281.

[26] P. B. Lourenço and J. Branco, "Dos abrigos da pré-história aos edifícios de madeira do século XXI," *História da Construção Arquiteturas e Técnicas Construtiva*, pp. 199–211, 2012, [Online]. Available: http://hdl.handle.net/1822/26503.

[27] G. J. Zenid, L. F. T. di Romagnano, M. A. R. Nahuz, M. J. de A. C. Miranda, O. P. Ferreira, and S. Brazolin, *Madeira: Uso sustentável na construção civil*, 2nd ed. São Paulo, 2009.

[28] G. C. A. Martins, "Análise Numérica e Experimental de vigas de Madeira Laminada Colada em Situação de Incêndio," Universidade de São Paulo - Escola de engenharia de São Carlos, 2016.

[29] O. Anjos, C. Rodrigues, J. Morais, and H. Pereira, "Effect of density on the compression behaviour of cork," *Mater. Des.*, vol. 53, pp. 1089–1096, Jan. 2014, doi: 10.1016/j.matdes.2013.07.038.

[30] M. Delucia, A. Catapano, M. Montemurro, and J. Pailhès, "Pre-stress state in cork agglomerates: simulation of the compression moulding process," *Int. J. Mater. Form.*, vol. 14, no. 3, pp. 485–498, May 2021, doi: 10.1007/s12289-021-01623-x.

[31] "Centro de Competências do Sobreiro e da Cortiça Promove Evento Dedicado às Diversas Fileiras do Montado," 2019. https://www.cap.pt/noticias-cap/agricultura-e-floresta/centro-de-competencias-do-sobreiro-e-da-cortica-promove-evento-dedicado-as-diversas-fileiras-do-montado (accessed Jul. 10, 2022).

[32] S. Knapic, V. Oliveira, J. S. Machado, and H. Pereira, "Cork as a building material: a review," *Eur. J. Wood Wood Prod.*, vol. 74, no. 6, pp. 775–791, Nov. 2016, doi: 10.1007/s00107-016-1076-4.

[33] H. Pereira, *Cork: Biology, Production and Uses*, 1st ed. Amsterdam, 2007.

[34] A. Antunes *et al.*, "Blocked melamine-urea-formaldehyde resins and their usage in agglomerated cork panels," *J. Appl. Polym. Sci.*, vol. 135, no. 35, p. 46663, Sep. 2018, doi: 10.1002/app.46663.

[35] S. P. Silva, M. A. Sabino, E. M. Fernandes, V. M. Correlo, L. F. Boesel, and R. L. Reis, "Cork: properties, capabilities and applications," *Int. Mater. Rev.*, vol. 50, no. 6, pp. 345–365, Dec. 2005, doi: 10.1179/174328005X41168.

[36] S. Kim, "A Study on Cork-based Plastic Composite Material," Massachusetts Institute of Technology, 2011.

[37] C. R. Sanquetta, G. M. Santana, M. N. I. Sanquetta, T. W. G. de Oliveira, and A. P. Dalla Corte, "Prudução, Importação, Exportação e Consumo Aparente de Painéis de Madeira no Brasil entre 1961 e 2016," *BIOFIX Sci. J. - Univ. Fed. do Paraná*, vol. 5, no. 1, pp. 44–49, Aug. 2020, doi: 10.5380/biofix.v5i1.66112.

[38] B. C. S. Ferreira, M. G. Firme, and N. O. Baldansi, "Uma proposta de uso da casca de café na confecção de painéis de madeira do tipo MDP," *Brazilian J. Dev.*, vol. 5, no. 7, pp. 10021–10027, 2019, doi: 10.34117/bjdv5n7-167.

[39] S. Iwakiri, "Painéis De Madeira," *UTFPR - DETF*, pp. 1–39, 2017.

[40] S. Iwakiri, J. L. M. de Matos, R. Trianoski, and J. G. Prata, "Produção de painéis aglomerados homogêneos e multicamadas de Melia azedarach (Cinamomo) e Pinus taeda com diferentes teores de resina," *CERNE*, vol. 18, no. 3, pp. 465–470, Sep. 2012, doi: 10.1590/S0104-77602012000300014.

[41] J. B. Paes, S. T. Nunes, F. A. R. Lahr, M. de F. Nascimento, and R. M. de A. Lacerda, "Qualidade de chapas de partículas de *Pinus elliottii* coladas com resina poliuretana sob diferentes combinações de pressão e temperatura," *Ciência Florest.*, vol. 21, no. 3, pp. 551–558, Sep. 2011, doi: 10.5902/198050983812.

[42] C. Sergi, J. Tirillò, F. Sarasini, E. B. Pozuelo, S. S. Saez, and C. Burgstaller, "The potential of agglomerated cork for sandwich structures: A systematic investigation of physical, thermal, and mechanical properties," *Polymers (Basel).*, vol. 11, no. 12, 2019, doi: 10.3390/polym11122118.

[43] C. Besse, "Development and Optimization of a Formable Sandwich Sheet," École Politechnique, 2012.

[44] F. Sarasini *et al.*, "Static and dynamic characterization of agglomerated cork and related sandwich structures," *Compos. Struct.*, vol. 212, no. January, pp. 439–451, Mar. 2019, doi: 10.1016/j.compstruct.2019.01.054.

[45] B. Källander and P. Lind, "Strength properties of wood adhesives after exposure to fire : Nordtest project no 1482-00," 2001.

[46] M. Klippel, A. Frangi, and M. Fontana, "Influence of the adhesive on the load-carrying capacity of glued laminated timber members in fire," *Fire Saf. Sci.*, pp. 1219–1232, 2011, doi: 10.3801/IAFSS.FSS.10-1219.

[47] P. T. Santos, S. Pinto, P. A. A. P. Marques, A. B. Pereira, and R. J. Alves de Sousa, "Agglomerated cork: A way to tailor its mechanical properties," *Compos. Struct.*, vol. 178, pp. 277–287, Oct. 2017, doi: 10.1016/j.compstruct.2017.07.035.

[48] X. C. Wang *et al.*, "Effects of expandable graphite on the flame-retardant and mechanical performances of rigid polyurethane foams," *J. Phys. Condens. Matter*, vol. 34, no. 8, 2022, doi: 10.1088/1361-648X/ac3b27.

[49] C. Chao, M. Gao, and S. Chen, “Expanded graphite,” *J. Therm. Anal. Calorim.*, vol. 131, no. 1, pp. 71–79, Jan. 2018, doi: 10.1007/s10973-016-6084-4.

[50] M. Thirumal, D. Khastgir, N. K. Singha, B. S. Manjunath, and Y. P. Naik, “Effect of expandable graphite on the properties of intumescent flame-retardant polyurethane foam,” *J. Appl. Polym. Sci.*, vol. 110, no. 5, pp. 2586–2594, Dec. 2008, doi: 10.1002/app.28763.

[51] D. K. Chattopadhyay and D. C. Webster, “Thermal stability and flame retardancy of polyurethanes,” *Prog. Polym. Sci.*, vol. 34, no. 10, pp. 1068–1133, 2009, doi: 10.1016/j.progpolymsci.2009.06.002.

[52] A. Strąkowska, S. Członka, P. Konca, and K. Strzelec, “New Flame Retardant Systems Based on Expanded Graphite for Rigid Polyurethane Foams,” *Appl. Sci.*, vol. 10, no. 17, p. 5817, Aug. 2020, doi: 10.3390/app10175817.

[53] Z. Zheng, Y. Liu, L. Zhang, and H. Wang, “Synergistic effect of expandable graphite and intumescent flame retardants on the flame retardancy and thermal stability of polypropylene,” *J. Mater. Sci.*, vol. 51, no. 12, pp. 5857–5871, 2016, doi: 10.1007/s10853-016-9887-6.

[54] A. Laachachi, N. Burger, K. Apaydin, R. Sonnier, and M. Ferriol, “Is expanded graphite acting as flame retardant in epoxy resin?,” *Polym. Degrad. Stab.*, vol. 117, pp. 22–29, Jul. 2015, doi: 10.1016/j.polymdegradstab.2015.03.016.

[55] S. Duquesne *et al.*, “Expandable graphite: A fire retardant additive for polyurethane coatings,” *Fire Mater.*, vol. 27, no. 3, pp. 103–117, 2003, doi: 10.1002/fam.812.

[56] M. R. M. Marinho, “Planejamento Fatorial: Uma Ferramenta Poderosa Para Os Pesquisadores,” *Congr. Bras. Ensino Eng.*, pp. 1–9, 2005.

[57] D. C. Montgomery, *Design and Analysis of Experiments*, 8ª ed. 2013.

[58] D. D. Siqueira, D. D. . S. Morais, E. M. Araújo, C. B. B. Luna, and R. M. R. Wellen, “Otimização da Funcionalização de um Polímero Biodegradável Utilizando Planejamento Fatorial,” vol. 3, no. 2017, pp. 192–198, 2018.

[59] W. M. Zeviani and F. de P. Mayer, "Experimentos fatoriais 2k," in *Controle de Processos Industriais*, Laboratório de Estatística e Geoinformação Departamento de Estatística Universidade Federal do Paraná, 2019.

[60] R. G. Drabeski, "Desenvolvimento de Filmes Finos de Dióxido de Estanho Depositados via Spin-Coationg e Caracterização das Propriedades Mecânicas e Termo-Ópticas," Universidade Tecnológica Federal do Paraná, 2019.

[61] F. C. Vicentini, L. C. S. Figueiredo-Filho, B. C. Janegitz, A. Santiago, E. R. Pereira-Filho, and O. Fatibello-Filho, "Planejamento fatorial e superfície de resposta: Otimizaç ão de um método voltamétrico para a determinaçã o de Ag(I) empregando um eletrodo de pasta de nanotubos de carbono," *Quim. Nova*, vol. 34, no. 5, pp. 825–830, 2011.

[62] F. S. V. C. B. Silva, V. L. da Silva, A. F. Lavorante, and A. P. S. Paim, "Utilização de planejamento fatorial no preparo de amostras de detergente em pó para a determinação de fósforo por análise em fluxo," *Quim. Nova*, vol. 33, no. 5, pp. 1199–1203, 2010, doi: 10.1590/s0100-40422010000500035.

[63] R. G. Drabeski, D. T. Dias, M. M. Moia, G. B. de Souza, E. T. Kubaski, and S. M. Tebcherani, "Crescimento de Camadas de Filmes Finos de SNO2 em Substrato de Vidro pale Técnica Spin Coating," 2018, doi: 10.29327/xxifisica.128807.

[64] E. M. Pinto, "Determinação de um Modelo de Taxa de Carbonização Transversal a Grã para o Eucalyptus citriodora E E. grandis," Universidade de São Paulo, 2005.

[65] E. V. M. Carrasco, R. B. Caldas, A. L. C. Oliveira, and R. H. Fakury, "Análise numérica da transferência de calor em madeiras brasileiras em situação de incêndio," in *CERNE*, 2010, vol. 16, pp. 58–65.

[66] CEN, "EN 13501-2:2016 (E) Fire classification of construction products and building elements - Part 2: Classification using data from fire resistance tests, excluding ventilation services," *Eur. Comm. Stand.*, 2016.

[67] O. S. Conde, "Reação ao Fogo de Elementos de Construção Leve com Incorporação Incorporação de Resísuos Têxteis," Instituto Politécnico de Bragança, 2020.

[68] CEN, *EN ISO 13927 - Plastics - Simple heat release test using a conical radiant heater and a thermopile detector*. 2003.

[69] B.-H. Lee *et al.*, "Evaluating the flammability of wood-based panels and gypsum particleboard using a cone calorimeter," *Constr. Build. Mater.*, vol. 25, pp. 3044–3050, Jul. 2011, doi: 10.1016/j.conbuildmat.2011.01.004.

[70] L. C. Ferle, "Análise da durabilidade das propriedades mecânicas e reação ao fogo dos painéis derivados de madeira," Instituto Politécnico de Bragança, 2018.

[71] F. Wang, J. Liu, and W. Lv, "Thermal degradation and fire performance of wood treated with PMUF resin and boron compounds," *Fire Mater.*, vol. 41, no. 8, pp. 1051–1057, 2017, doi: 10.1002/fam.2445.

[72] X. Liu *et al.*, "The preparation of a bisphenol A epoxy resin based ammonium polyphosphate ester and its effect on the char formation of fire resistant transparent coating," *Prog. Org. Coatings*, vol. 129, no. November 2018, pp. 349–356, 2019, doi: 10.1016/j.porgcoat.2019.01.003.

[73] N. Z. M. Zuhudi, R. J. T. Lin, and K. Jayaraman, "Flammability, thermal and dynamic mechanical properties of bamboo-glass hybrid composites," *J. Thermoplast. Compos. Mater.*, vol. 29, no. 9, pp. 1210–1228, 2016, doi: 10.1177/0892705714563118.

[74] P. B. Cachim and J.-M. Franssen, "Comparison between the charring rate model and the conductive model of Eurocode 5," *Fire Mater.*, vol. 33, no. 3, pp. 129–143, Apr. 2009, doi: 10.1002/fam.985.

[75] J. A. Silva, B. P. G. D. L. Damasceno, F. L. H. da Silva, M. S. Madruga, and D. P. de Santana, "Aplicação da metodologia de planejamento fatorial e análise de superfícies de resposta para otimização da fermentação alcoólica," *Quim. Nova*, vol. 31, no. 5, pp. 1073–1077, 2008, doi: 10.1590/S0100-40422008000500024.

[76] L. Moreira, V. A. F. Costa, and F. Neto da Silva, "Effect of moisture content on curing kinetics of agglomerate cork," *Mater. Des.*, vol. 82, pp. 312–316, 2015, doi: 10.1016/j.matdes.2015.01.001.

[77] F. M. C. Martins, "Aglomeração de cortiça por compressão a quente glomeração de cortiça por compressão a quenteA," Instituto Superior de Engenharia do Porto, 2015.

[78] R. Ferreira, D. Pereira, A. Gago, and J. Proença, "Experimental characterisation of cork agglomerate core sandwich panels for wall assemblies in buildings," *J. Build. Eng.*, vol. 5, pp. 194–210, Mar. 2016, doi: 10.1016/j.jobe.2016.01.003.

[79] N. Lakreb, N. As, V. Gorgun, U. Sen, M. G. Gomes, and H. Pereira, "Production and characterization of particleboards from cork-rich Quercus cerris bark," *Eur. J. Wood Wood Prod.*, vol. 76, no. 3, pp. 989–997, May 2018, doi: 10.1007/s00107-017-1284-6.

[80] K. Crouvisier-Urion, J. P. Bellat, R. D. Gougeon, and T. Karbowiak, "Mechanical properties of agglomerated cork stoppers for sparkling wines: Influence of adhesive and cork particle size," *Compos. Struct.*, vol. 203, pp. 789–796, 2018, doi: 10.1016/j.compstruct.2018.06.116.

[81] M. Delucia, A. Catapano, M. Montemurro, and J. Pailhès, "Determination of the effective thermoelastic properties of cork-based agglomerates," *J. Reinf. Plast. Compos.*, vol. 38, no. 16, pp. 760–776, 2019, doi: 10.1177/0731684419846991.

[82] M. E. Dagort, "Desenvolvimento de um Sistema Multicamada de Madeira e Derivados de Madeira Resistente ao Fogo," Instituto Politécnico de Bragança com a Universidade Tecnológica Federal do Paraná, 2022.

[83] OriginLab Corporation, "OriginPro." Northampton, MA, USA.

[84] CEN, *EN 1363-1 Fire resistance tests - Part 1: General requirements*. 2020.

Attachments

Attachment I – MATLAB code to calculate the necessary parameters for the manufacture of each agglomerated cork panel.

```
clear
 close all;
 clc;
  % Input:
 density_kgm3 = 0;
 lenght_mm = 0;
 mould_area_m2 = 0;
 % Output:
 pressure_kPa = 0;
 press_force_kN = 0;
 cork_quantity_3_4mm_g = 0;
 cork_quantity_02_05mm_g = 0;
 % Pressure
   %origin equation density x pressure
    %   ->   density = 111.82973 + 1.27624*pressure
     %   ->   density = a + b*pressure
      %   ->   pressure = (density - a)/b
a=111.82973;
b=1.27624;
pressure_kPa = (density_kgm3 - a)/b;
```

```
% Press Force to be Applied

press_force_kN = pressure_kPa*mould_area_m2;

% Compress Ratio

 %origin equation compression ratio x pressure

   %   ->   compression ratio = 1.7658 + 0.01962*pressure

    %   ->   compression ratio = a2 + b2*pressure

a2 = 1.7658;

b2 = 0.01962;

compress_ratio = a2 +b2*pressure_kPa;

% Volumes

final_volume_m3 = mould_area_m2*lenght_mm*(10^(-3));

initial_lenght_mm = lenght_mm*compress_ratio;

initial_volume_m3 = mould_area_m2*initial_lenght_mm*(10^(-3));

% Cork Quantity

cork_3_4_mm_density_kgm3 = 55;

cork_02_05_mm_density_kgm3 = 90;

cork_quantity_3_4mm_g = initial_volume_m3*cork_3_4_mm_density_kgm3*(10^3);

cork_quantity_02_05mm_g = cork_quantity_3_4mm_g*(7.3508/123.3293);

% Resin Quantity

resin_quantity_g = (cork_quantity_02_05mm_g + cork_quantity_3_4mm_g)*0.1;

% Water Quantity

water_quantity_g_if_MDI = (cork_quantity_02_05mm_g + cork_quantity_3_4mm_g +
resin_quantity_g)*0.21;

water_quantity_g_if_TDI = (cork_quantity_02_05mm_g + cork_quantity_3_4mm_g +
resin_quantity_g)*0.14;

% EG Quantity

EG_5_quantity_g = (cork_quantity_02_05mm_g + cork_quantity_3_4mm_g +
resin_quantity_g)*(5/95);
```

EG_10_quantity_g = (cork_quantity_02_05mm_g + cork_quantity_3_4mm_g + resin_quantity_g)*(10/90);

EG_20_quantity_g = (cork_quantity_02_05mm_g + cork_quantity_3_4mm_g + resin_quantity_g)*(20/80);

Attachment II – Table of panel mix component quantities.

Sample Name	Cork Mass (g)		Resin Mass (g)	Water Mass (g)	EG Mass (g)
	3-4 mm	0,2-0,5 mm			
MDI-12mm-0%EG	500.4	29.8	53.0	122.5	-
MDI-19mm-0%EG	792.3	47.2	83.9	193.9	-
MDI-19mm-5%EG	792.3	47.2	83.9	193.9	48.6
MDI-19mm-10%EG	792.3	47.2	83.9	193.9	102.6
MDI-19mm-20%EG	792.3	47.2	83.9	193.9	230.9
TDI-12mm-0%EG	500.4	29.8	53.0	81.6	-
TDI-19mm-0%EG	792.3	47.2	83.9	129.3	-
TDI-19mm-5%EG	792.3	47.2	83.9	129.3	48.6
TDI-19mm-10%EG	792.3	47.2	83.9	129.3	102.6
TDI-19mm-20%EG	792.3	47.2	83.9	129.3	230.9